

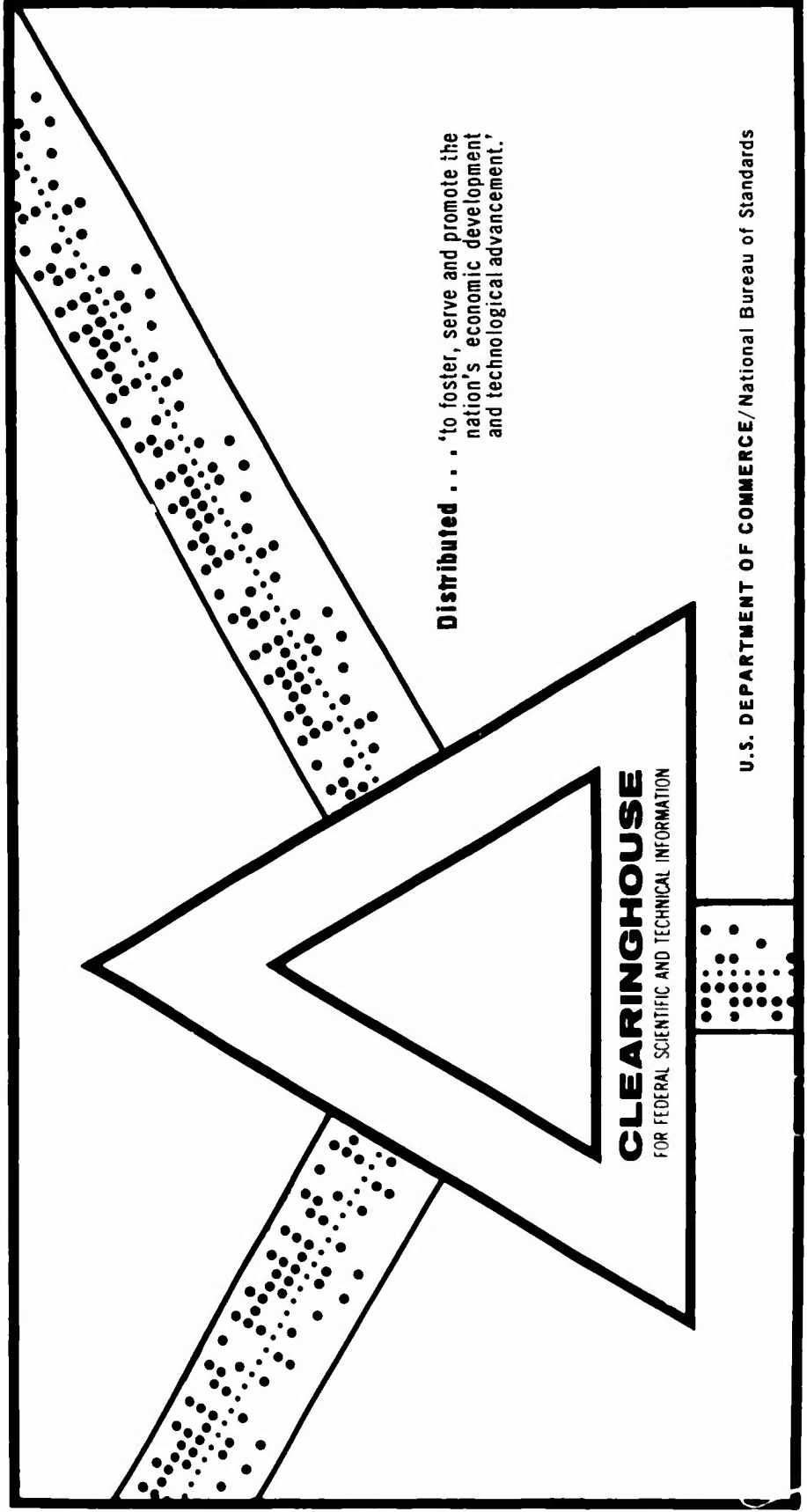
AD 696 997

STUDIES IN MARINE GEOPHYSICS AND UNDERWATER SOUND FROM DRIFTING
ICE STATIONS

Kenneth L. Hunkins, et al

Lamont-Doherty Geological Observatory
Palisades, New York

September 1969



Distributed . . . to foster, serve and promote the
nation's economic development
and technological advancement.

CLEARINGHOUSE
FOR FEDERAL SCIENTIFIC AND TECHNICAL INFORMATION

U.S. DEPARTMENT OF COMMERCE/National Bureau of Standards

This document has been approved for public release and sale.

AD 696997

Lamont-Doherty Geological Observatory
of
Columbia University
Palisades, New York 10964

STUDIES IN MARINE GEOPHYSICS AND
UNDERWATER SOUND FROM DRIFTING ICE STATIONS

by

Kenneth L. Hunkins
Henry W. Kutschale
John K. Hall

Final Report

Nonr 266(82)

Research Supported by the Office
of Naval Research and the
Advanced Research Projects Agency

DDC
NOV 21 1969

Reproduction of this document in whole or in part is permitted
for any purpose of the U. S. Government.

September 1969

This document has been approved
for public release and sale; its
distribution is unlimited

Reproduced by the
CLEARINGHOUSE
for Federal Scientific & Technical
Information Springfield Va 22151

107

LAMONT-DOHERTY GEOLOGICAL OBSERVATORY OF COLUMBIA UNIVERSITY

Palisades, New York

STUDIES IN MARINE GEOPHYSICS AND UNDERWATER SOUND
FROM DRIFTING ICE STATIONS

by

Kenneth L. Hunkins
Henry W. Kutschale
John K. Hall

Final Report

Nonr 266(82)

Research by _____
of Naval Research and Development
Advanced Research Projects Agency

Reproduction of this document in whole or in part is permitted for any
purpose of the U. S. Government

September 1969

TABLE OF CONTENTS

	Page
Introduction	1-2
Narrative of Lamont Activities on the Ice Stations - Kenneth L. Hunkins	2-10
Hydroacoustics - Henry W. Kutschale	11-26
References	27-28
Captions for Figures	29-32
Figures	
Geophysical Investigation from Fletcher's Ice Island - John K. Hall	33-44
Abstracts of Selected Papers and Reports Issued Under Contract NONR 266 (82)	45-64
Bibliography of Scientific Papers Supported Under Contract NONR 266 (82)	65-68
Technical Reports Issued Under Contract NONR (266)82	69
Encyclopedia Articles and Other	70

Introduction

The Arctic Ocean was still a relatively unexplored area in 1961. The International Geophysical Year had resulted in much new data, but many new questions about Arctic geophysics and oceanography had been posed by the new information gained. In order to fill the continuing need for basic information concerning marine geophysics and underwater acoustics in this ocean, the Office of Naval Research contracted with the Lamont Geological Observatory to carry out a program of fundamental oceanographic research from drifting ice stations. Drifting ice stations are semi-permanent camps established on ice floes or ice islands. These stations offer several advantages for research. They are uniquely stable platforms, drifting with the winds and ocean currents. From them, all the types of measurements taken from oceanographic research vessels may be conducted. The Lamont group had acquired experience on drifting ice stations under Air Force support from 1957 to 1961 when research was done at stations Alpha, Charlie, and T-3.

Two ice stations were utilized for the work done under this contract. Research was conducted at Arlis II during the summer of 1961 and 1962. In the spring of 1962 a program of marine geophysics and physical oceanography was established on Fletcher's Ice Island (T-3). T-3 had been abandoned by the Air Force after

it grounded on the continental shelf northwest of Point Barrow. Sometime during the winter of 1961-62, it drifted free and was reoccupied by an Arctic Research Laboratory crew in early 1962. A basic research program was hastily organized at Lamont after the reoccupation of T-3 and by May of that year depth soundings and magnetic and gravity observations were being made. The Lamont program was the first research program to be reestablished on T-3. This program has operated continuously at T-3 since that time. A party of two to four scientists and technicians has constantly operated the program through the polar winters and polar summers of seven years. Table I lists the individuals participating in the field program and the dates of their duty tours. The simple program of 1962 has been improved continuously until at present the program at T-3 is as sophisticated as any on a modern oceanographic research vessel in other oceans. Today T-3 supports such equipment as the Navy Satellite Navigation System, a Precision Depth Recorder, a seismic profiler, proton free-precession magnetometer, and many other items, all as a part of the Lamont program.

Narrative of Lamont Activities on the Ice Stations

1. Arlis II

During the summer of 1961, Henry Kutschale carried out a program of seismic and underwater acoustic experiments. An extensive study of the island ice of Arlis II was made using various types

TABLE I

3.

LAMONT-DOHERTY PERSONNEL ON FLETCHER'S ICE ISLAND (T-3) 1961-1969

ALBERINO, JAMES J.	04/06/62-17/09/62		
ALLEN, L. BARRY	07/06/64-30/09/64	04/06/66-29/09/66	16/02/67-02/06/67
ALONSO, DIEGO	26/09/68-30/01/69		
AMBROSIO, FRANK F.	27/11/62-10/03/63		
BERRY, JOHN L.	17/06/63-15/09/63		
BOGAERTS, WINOC F.	20/01/63-15/05/63		
BROCOUM, STEPHAN J.	04/03/63-05/06/63		
BURGER, JOHN R.	23/09/65-05/01/66		
COCHEO, RICHARD N.	22/09/65-18/02/66	25/02/66-23/04/66	25/04/66-22/05/66
COTTONE, JAMES F.	04/10/62-26/11/62		
COURTNEY, ROBERT H. III	18/05/67-16/09/67		
DAVIS, EDWARD E.	05/06/65-30/09/65		
FELDMAN, MARVIN L.	22/09/66-02/02/67		
FRIEDMAN, ROBERT M.	18/02/64-24/05/64		
GILL, ALLAN	23/02/64-05/06/64	29/09/64-22/03/65	18/10/65-29/04/66
HALL, JOHN K.	30/05/66-08/10/66	16/03/67-21/09/67	25/09/68-28/10/68
HUNKINS, KENNETH L.	08/05/62-01/06/62	30/05/63-01/10/63	03/04/67-17/05/67
	27/04/68-21/05/68		
JOKELA, ARTHUR W.	29/09/62-20/01/63		
KUTSCHALE, HENRY W.	30/03/68-23/05/68		
LARDER, DAVID J.	28/12/67-06/05/68		
LAW, GRAHAM D.	06/06/69-		
LIU, PETER Y. C.	04/06/67-09/09/67		
LOUCHE, WILLIAM A.	23/05/68-26/09/68		
MATHIEU, GUY G.	18/05/66-29/09/66	06/03/67-02/06/67	30/03/68-27/05/68
	19/04/69-04/05/69		
MCHAIR, DONALD W.	22/05/64-17/09/64		
NITSAN, UZI	12/06/68-26/09/68		
PAGE, ROBERT A., JR.	06/06/61-19/09/61		
PALMER, PAUL W.	12/09/67-01/03/68		
REHQUATE, RUDOLF E.	17/09/63-22/12/63		
RICE, ERIC A.	15/09/63-17/03/64	05/06/65-23/09/65	
RICE, PATRICK A.	29/09/64-14/01/65		
SCHOEN, LEON J.	12/09/67-26/01/68	11/01/69-28/05/69	
SHAVER, RALPH N.	24/05/62-04/10/62	09/10/62	16/05/63-26/09/63
	05/11/64-20/11/64	12/02/65-21/02/65	
SPARTIS, JAMES A.	27/04/69-13/06/69		
TEETER, STEVEN R.	30/09/68-06/05/69		
TIEMANN, WERNER W. JR.	12/01/65-04/06/65	03/10/66-15/02/67	01/03/68-08/06/68
WALKER, JAMES C. G.	01/06/61-19/09/61		
WILKINS, ROBERT C.	05/03/65-11/06/65		
WILLINSKI, GARY A.	06/06/69-		
YEARSLEY, JOHN R.	16/09/63-21/12/63		

LAMONT-DOHERTY PERSONNEL ON ICE ISLAND ARLIS II 1961-1962

KUTSCHALE, HENRY W.	15/04/61-30/10/61	10/04/62-04/10/62
PRENTISS, DAVID D.	07/04/62-20/05/62	
RASMUSSEN, GERALD E.	02/06/62-26/09/62	

of elastic waves. Investigation was made of the propagation of flexural, air-coupled flexural, longitudinal, transverse and Crary waves through the ice. Different propagation characteristics were noted for the two types of ice which compose the island. The ice types, called blue and gray, have their origin as ice shelves and sea ice respectively and differ in their thickness and elastic properties. Arlis II was a composite of the two types.

Seismic shooting for ocean depth and sub-bottom structure was also conducted on a daily basis. Successful seismic refraction and long range acoustic experiments were also made during the summer with the icebreaker U.S.S. Staten Island as shooting ship. Ground waves were recorded which showed a deep layer with a velocity of 7.35 km/sec. The shots were also recorded at Point Barrow by a group from the Universities of Wisconsin and Minnesota in a cooperative effort. The water waves provide new information on shallow-water transmission in the Arctic Ocean to ranges of 234 km.

A large Russian nuclear blast was recorded at Arlis II on October 23, 1961 with seismometers on the ice surface. A classified report on the detection of this blast was issued under this contract.

During April and May of 1962, measurements of acoustic noise on the floor of the Arctic Ocean were made from Arlis II. Henry

Kutschale and Dave Prentiss completed three stations on the ocean floor with a specially constructed bottom seismometer. The instrument consisted of a 2 Hz geophone, a transistorized amplifier, FM modulator and acoustic transmitter mounted in an aluminum pressure case. Data were telemetered acoustically to a hydrophone pickup near the surface. The noise levels on the ocean floor were found to be of the same order as those present at quiet continental locations. Ice vibrations on Arlis II itself were also measured with the same instrument. The results cover the frequency range of 0.1 to 100 cps and show an amplitude minimum between 6 and 10 cps and a maximum between 30 and 70 cps. Under the quietest conditions, Arlis II was seismically quieter than a quiet land site. Under the most unfavorable conditions, ice vibrations approached those at noisy land sites.

Sound transmission experiments were conducted between Arlis II and T-3. The paths between the stations changed as the two stations drifted. Signals with varying percentages of deep and shallow-water path were recorded. The deep water paths showed an intensification of the higher modes which had been suppressed by any appreciable portion of shallow-water path.

A seismic profiler utilizing both explosives and a sonar boomer as sound sources was operated on Arlis II in 1962. A magnetometer and precision depth recorder were also maintained. The Wrangel Abyssal Plain was explored geophysically during this period.

Bottom dredges and bottom cores were raised from the ocean floor during 1962.

2. Fletcher's Ice Island (T-3)

After the rediscovery of T-3 in February 1962 by the Arctic Research Laboratory airplane, a camp was reestablished. The Lamont group responded to a need for a scientific program on the station by quickly organizing a modest geophysical program. This program covered navigation, depth sounding, magnetic and gravity field measurements. During the summer of 1962, T-3 experienced a very rapid drift covering the entire length of the Chukchi Rise from south to north. The Chukchi Rise is apparently a fractured portion of continental shelf which has been moved into the ocean basin. For this reason it holds important clues to the origin of the Arctic Basin. The geophysical data from this summer drift added much to the knowledge of this feature. A minimum depth of 285 meters was recorded on 8 August. By 9 September, T-3 had drifted over the northwestern flank of the cap and was over water depths of 3000 meters. The prominent magnetic anomaly previously discovered over the western and northern flanks of the Chukchi Cap was further delineated.

About 120 explosive charges ranging from $\frac{1}{2}$ lb to 50 lb of TNT were detonated at depths of 100 to 2000 feet below T-3. These charges were fired in support of the Arctic SOPAR program

which was carried on between T-3 and Arlis II.

For a few weeks in the fall of 1962 the geomagnetic field intensity was measured simultaneously on T-3 and at a depth of 1000 feet below the ice island with a proton free-precession magnetic gradiometer constructed especially for the project by Varian Associates of Palo Alto, California. Data were recorded both on analog records and magnetic tape. The magnetic gradient was observed to vary as the ice station drifted over different geological structures. The gradiometer proved to be an effective instrument for discriminating between ionospheric and geological effects on the magnetic field since geological structures produced much stronger gradients. Analysis of the time variations and their attenuation with depth was made.

The basic program in geophysics continued through the winter with a crew of two.

An expanded program of research at T-3 was inaugurated in June 1963. One of the most significant additions to the program was a Precision Depth Recorder giving continuous rather than spot soundings. The station drifted over both the Alpha Cordillera and the Canada Abyssal Plain during this period and the PDR was effective in giving detailed topographic data.

Physical oceanographic studies were begun during this period. Continuous current measurements were made at three levels with

Roberts current meters. A program of serial hydrographic stations was begun. Bottom currents were measured with a photographic meter. Also a radiochemical sampling program of Arctic Ocean water was started. Water samples were taken from the surface, 75 m, 500 m, and 2000 m levels for radiocarbon analysis. Bottom sediment samples were also obtained for radiocarbon analysis. A seven barrel corer was used.

Bottom photography was also undertaken as a regular program with a Thorndike bottom camera.

Surface wave motions and earthquake wave trains were investigated on T-3. Three long period seismometers were established on the ice island in a triangular array. The object was to determine the direction of origin and the speed of long waves in the Arctic Ocean. A number of earthquakes were also detected.

Hunkins participated in a seismic refraction experiment in the Arctic Ocean during October and November of 1963. He recorded 109 shots in the Chukchi Sea while aboard the icebreaker U.S.C.G. Northwind. The U.S.S. Staten Island was the shooting ship.

During 1964, 1965 and the first part of 1966, T-3 drifted southward over the Canada Abyssal Plain. Depths varied little, remaining for the most part between 3700 and 3800 m. During this period, several new programs were introduced.

An investigation of internal waves was begun by John Yearsley using an array of thermistors suspended at depth. Hydro-

graphic stations supplemented the thermistor recordings.

A nephelometer was put into service at T-3 for measuring light scattering as a function of depth in the Arctic Ocean.

On 27 August 1966, T-3 drifted over the Northwind Cap and commenced a highly interesting course which carried it also across the Chukchi Rise, the Chukchi Abyssal Plain, and the Mendeleev Ridge. A spark-type seismic profiler was put into operation in time for delineating the sub-bottom structure of these features.

The fixing of T-3's position was vastly improved when a Radio Navigation Set, AN/SRN-9, was installed on April 14, 1967. This set provides access to the Navy Navigation Satellite System. Fixes are not only more accurate than the celestial fixes but, perhaps more important, they are obtained more often. The Navy Navigation Satellite System is a world-wide, all-weather system that provides accurate navigational fixes from data collected during a single pass of a polar-orbiting satellite. This system revolutionized positioning for T-3 for all scientific purposes. The improved positions aid greatly in the interpretation of all geophysical data collected during the drift. In addition, in the case of ice drift and current studies, it makes available details never before observed.

A vertical string of Savonius current meters at four depths down to 300 m was installed as one corner of a tripartite array

of thermistors at the same four levels. The system was designed to study the dynamics of the upper Arctic Ocean. The stable ice platform of T-3 provides a unique location for observing detailed motions of the upper layers. The satellite navigator was an essential element of this system since without knowledge of ice drift, data reduction would not be possible.

During 1968 the ice island crossed the Canada Abyssal Plain and moved over the Alpha Cordillera where it has continued to drift until the present time.

HYDROACOUSTICS

INTRODUCTION

The two unique features of the polar environment which most strongly influence underwater sound are the permanent ice cover and the velocity structure in the water. Ice movement generates background noise and the ice modifies propagation, particularly at high frequencies by scattering waves from the rough ice boundaries. Sound velocity is a function of temperature, salinity, and pressure. The relationship among these variables in the central Arctic Ocean is such that sound velocity is generally an increasing function of depth from the surface to the bottom. Such a velocity profile is found only in polar waters. The sound velocity structure is remarkably uniform both as a function of location and time of year. Sounds are transmitted to great ranges in this natural Arctic waveguide or sound channel by upward refraction in the water and repeated reflection from the ice canopy. A two-pound explosion of TNT has been heard at ranges exceeding 1100 km (700 miles). The surface sound channel of the Arctic is the polar extension of the deep sound channel or SOFAR channel of the nonpolar oceans (Ewing and Worzel 1948), but the character of the Arctic signals is often quite different from those observed in the deep channel, largely because of the predominance of low-

frequency waves in the Arctic. The Arctic sound channel is of considerable importance to the Navy because of the possibility of long-range detection and communication. This ocean also provides an ideal test area for new concepts of signal detection and processing because of the easy access to the sound channel and the permanence of installations located on ice islands.

Drifting ice stations provide an ideal platform for research on underwater sound. These stable platforms over deep or shallow water are far removed from ship traffic and they provide a large surface area for detector arrays. Detectors may be either seismometers mounted on the ice or hydrophones suspended at shallow depths in the water. Measurements of background noise and scattering layers may be made over periods of many years as the ice station moves slowly under the influence of winds and currents. Experiments on propagation are commonly made between two ice stations or between an ice station and an ice breaker or an aircraft. The latter type of experiment is particularly suited to measure the range dependence of the sound field and to determine the effects of bottom topography on the propagation.

High explosives have been the principal sound sources for transmission experiments. These sources radiate high sound intensity over a broad frequency range and they are easy to launch. Offsetting these advantages is the change of source spectrum with shot depth at constant charge size, occasional partial detonations,

Fig. 1

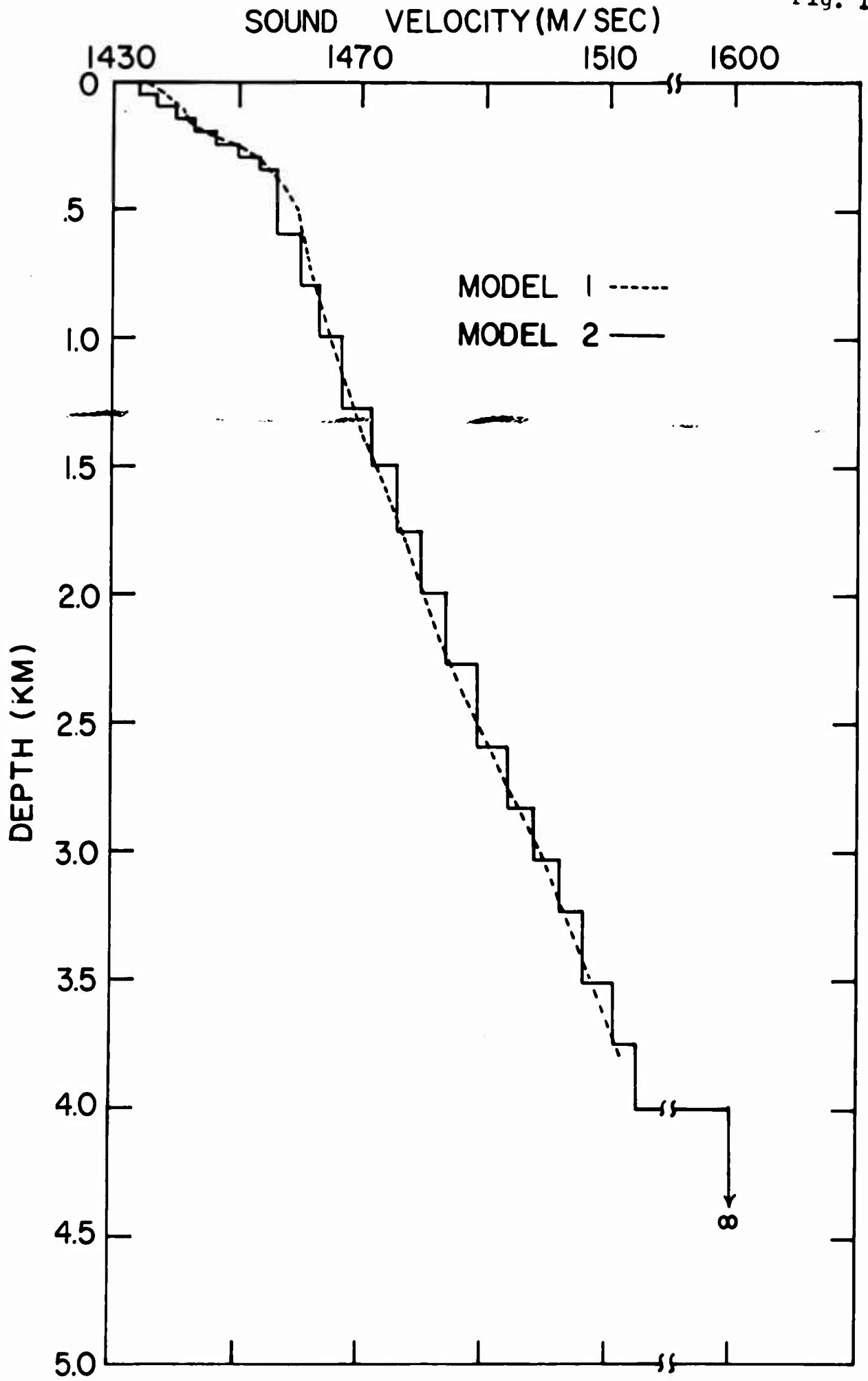
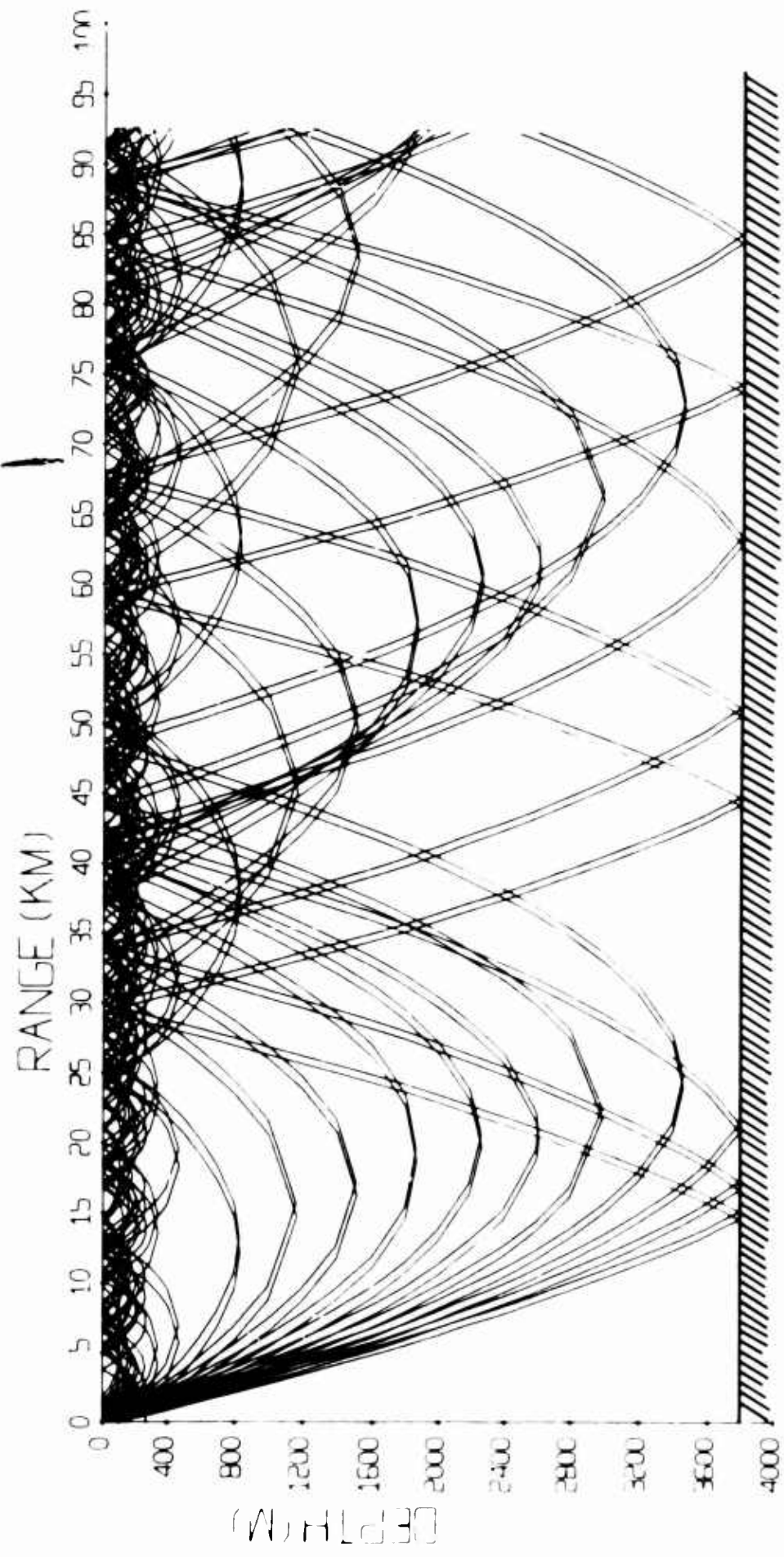


Fig. 2



and some variation of firing depth for pressure activated charges dropped from an aircraft. Also, detailed comparisons of theoretical computations with measurements are often far more difficult than for constant frequency sound sources.

Propagation

Many aspects of sound propagation in the Arctic Ocean may be understood in terms of ray theory, but at long ranges where low-frequency waves predominate, the solution of the wave equation in terms of normal modes is a powerful method for describing the propagation in detail. Figure 1 shows sound-velocity profiles which closely follow observed ones. Model 1 consists of a sequence of plane parallel layers, each layer having a constant velocity gradient. Such a model is convenient for numerical computations by ray theory. Model 2 represents the continuous variation of velocity and density with depth by a series of flat-lying layers of constant velocity and density. This representation is extremely useful for solving the wave equation when solid layers as well as liquid layers must be considered. The ice sheet is represented by a 3-m thick layer with the appropriate compressional velocity, shear velocity, and density. In the deep ocean the bottom sediments are represented by a liquid half-space, but in shallow water it may be necessary to represent the bottom by a layered solid.

Figure 2 shows ray paths from a source 100 m deep for Model 1 over the Canada Abyssal Plain in 3800 m of water. The concentration of rays near the axis of the channel is apparent. The

paths were computed by high-speed digital computer. The first refracted and surface-reflected (RSR) sound to arrive at a detector corresponds to the ray which has penetrated the deepest into the channel. As time progresses, successively shallower penetrating sounds arrive, each one corresponding to one more surface reflection than the preceding one. The RSR sounds arrive with increasing frequency until they terminate with the arrival of the sound which leaves the source in a horizontal direction. If the detector is deeper than the source, the last RSR sound is the one which arrives from a horizontal direction. In general, the sounds arrive in groups of four because of reflection near the source and the detector. There may be exceptions to this simple pattern for sounds traveling near the axis of the channel because of rather sharp changes in the velocity gradient in the upper 400 m of water. The bottom-reflected sounds are generally interspersed between the RSR sounds and they may continue long after the last RSR sound has passed. They arrive with decreasing frequency as a function of time and they also arrive in groups of four for a source and a detector at different depths. As the range increases, the number of sounds traveling by both types of paths increases correspondingly and so does the total duration of the signal. Sounds reflected by the boundaries of the channel are scattered and therefore weakened. This effect is particularly

Fig. 3

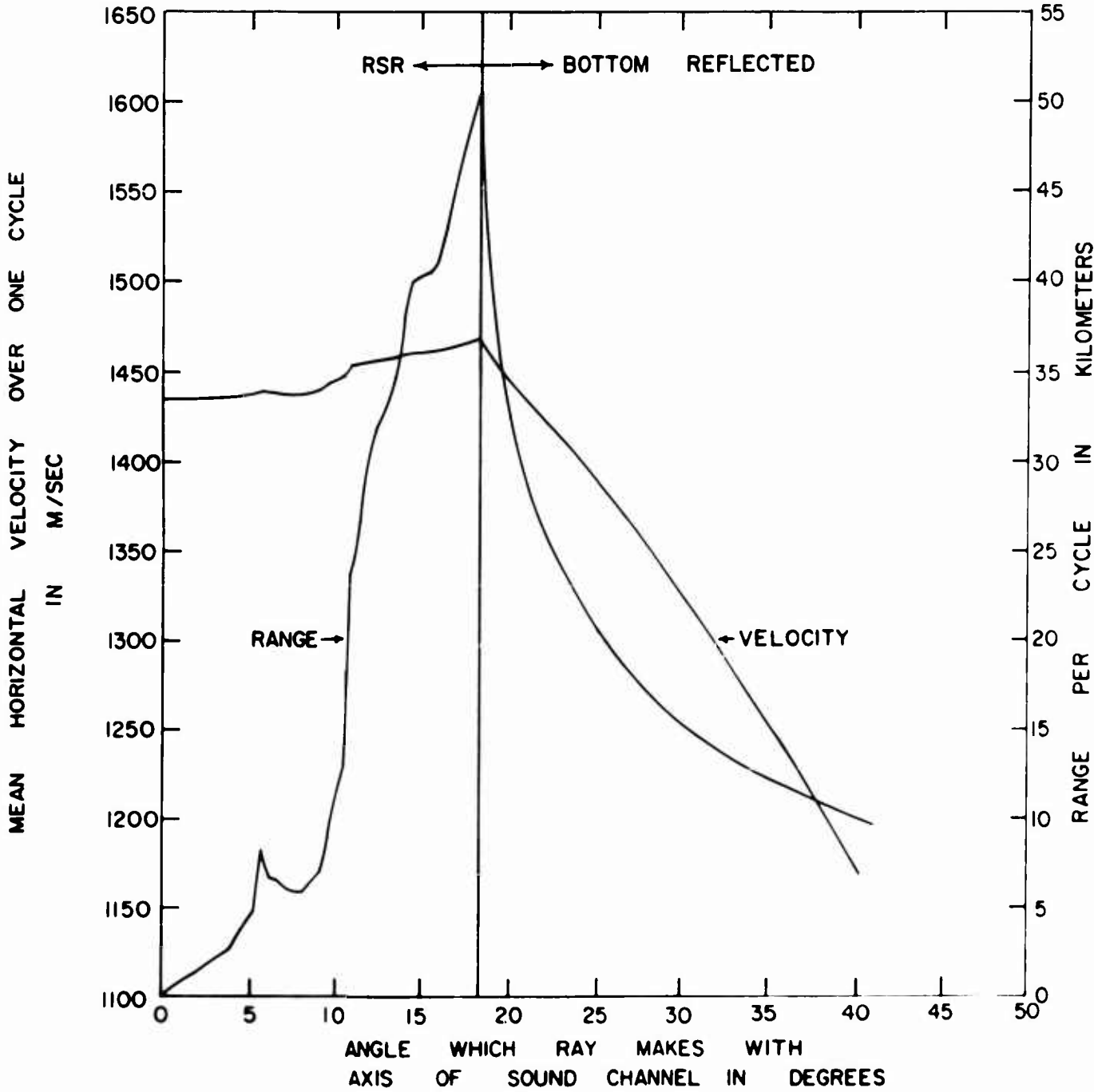
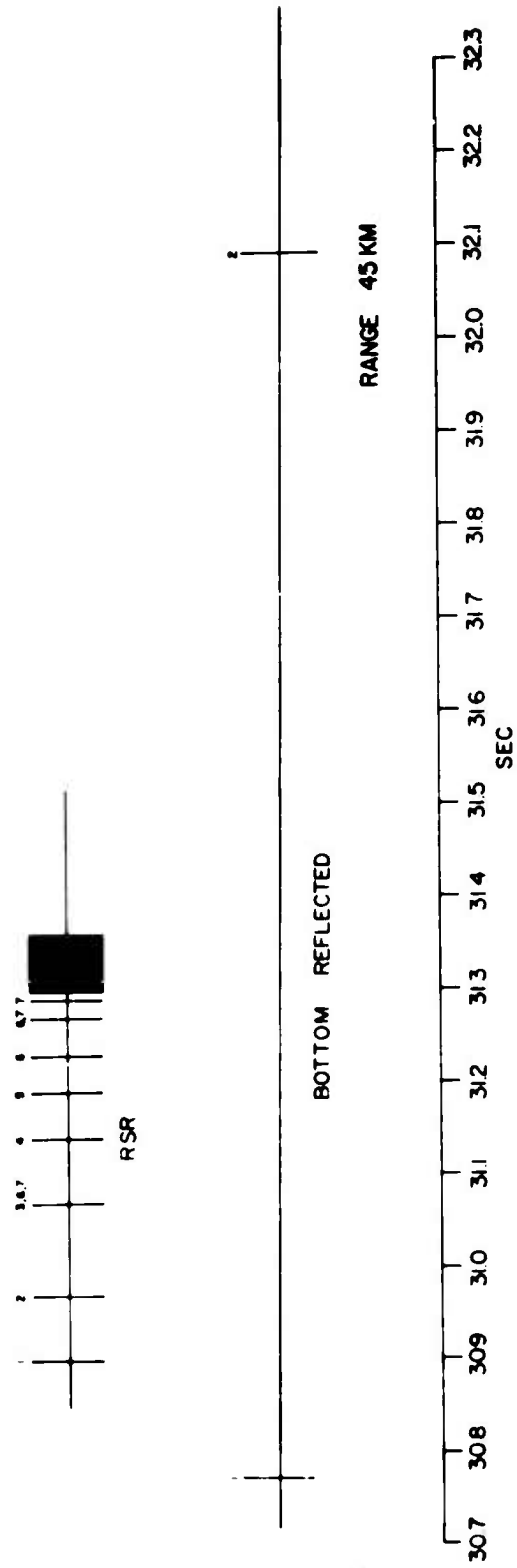


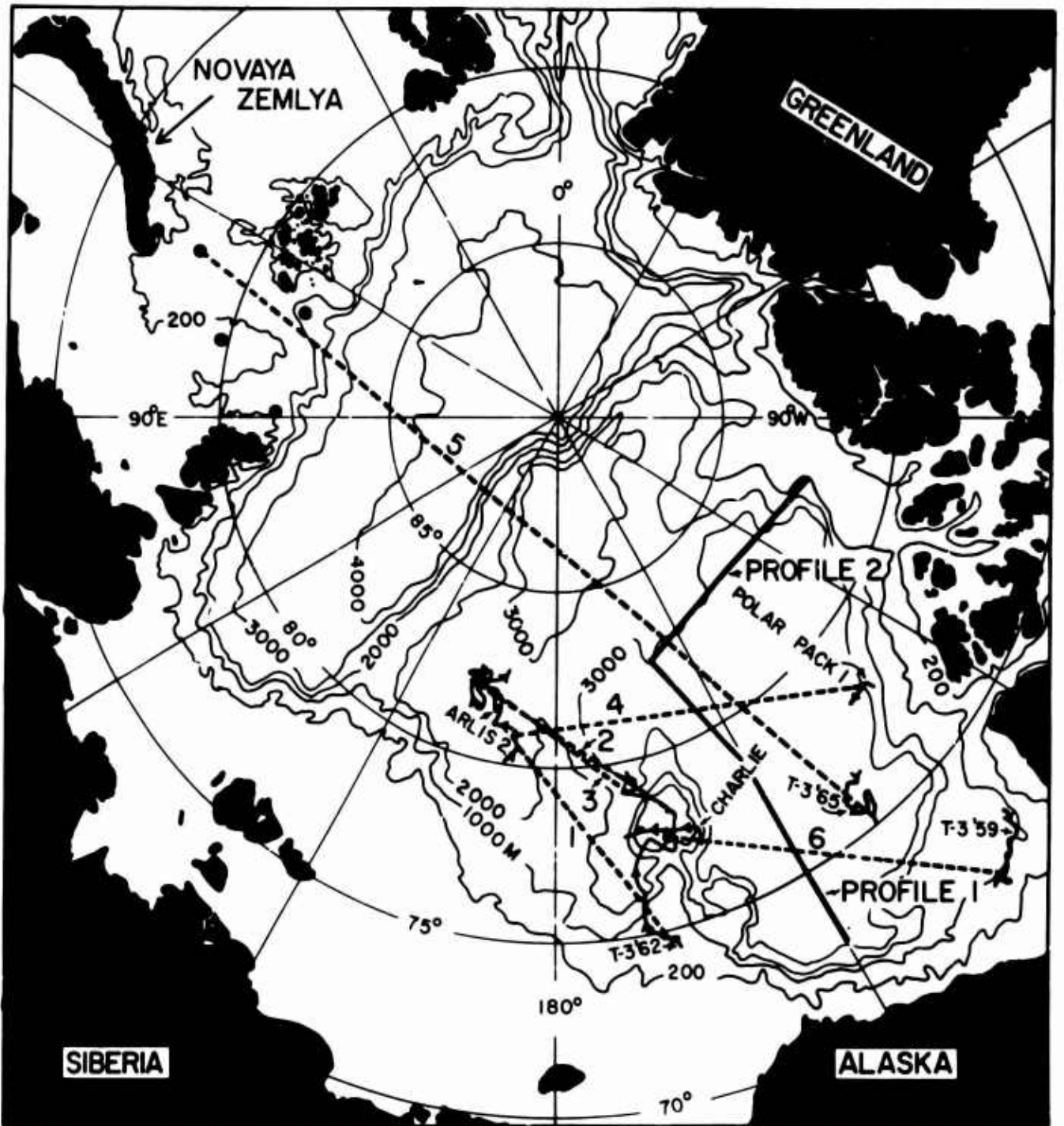
Fig. 4



strong for sounds reflected from the ocean bottom because of the very much larger scale of irregularities there than at the ice surface. Except for signals traveling over abyssal plains, the bottom-reflected sounds have a noncoherent character and they are weak compared with sounds traveling by RSR paths. The first strong sound generally corresponds to the ray which has passed over all bottom topography without striking the bottom.

Any two rays which make the same angle with the axis of the sound channel differ only by a horizontal displacement. The time sequence of sounds traveling by different paths may be determined by graphs like those of Figure 3 which give the range per cycle and the mean horizontal velocity over one cycle of a ray as a function of the angle the ray makes with the axis of the sound channel (grazing angle). An example of the sequence of arrivals is given in Figure 4 for a surface source and a surface detector separated by a range of 45 km. The number of cycles a ray has made is shown in the figure. There is a duplication or triplication of travel times for rays departing a surface source at angles between four and ten degrees. At these angles the signal strength is enhanced because of focusing of sounds by the relatively strong changes in the velocity gradient in the upper 400 m of water. At long ranges and low frequencies a regular oscillatory wave train is the result of interference of

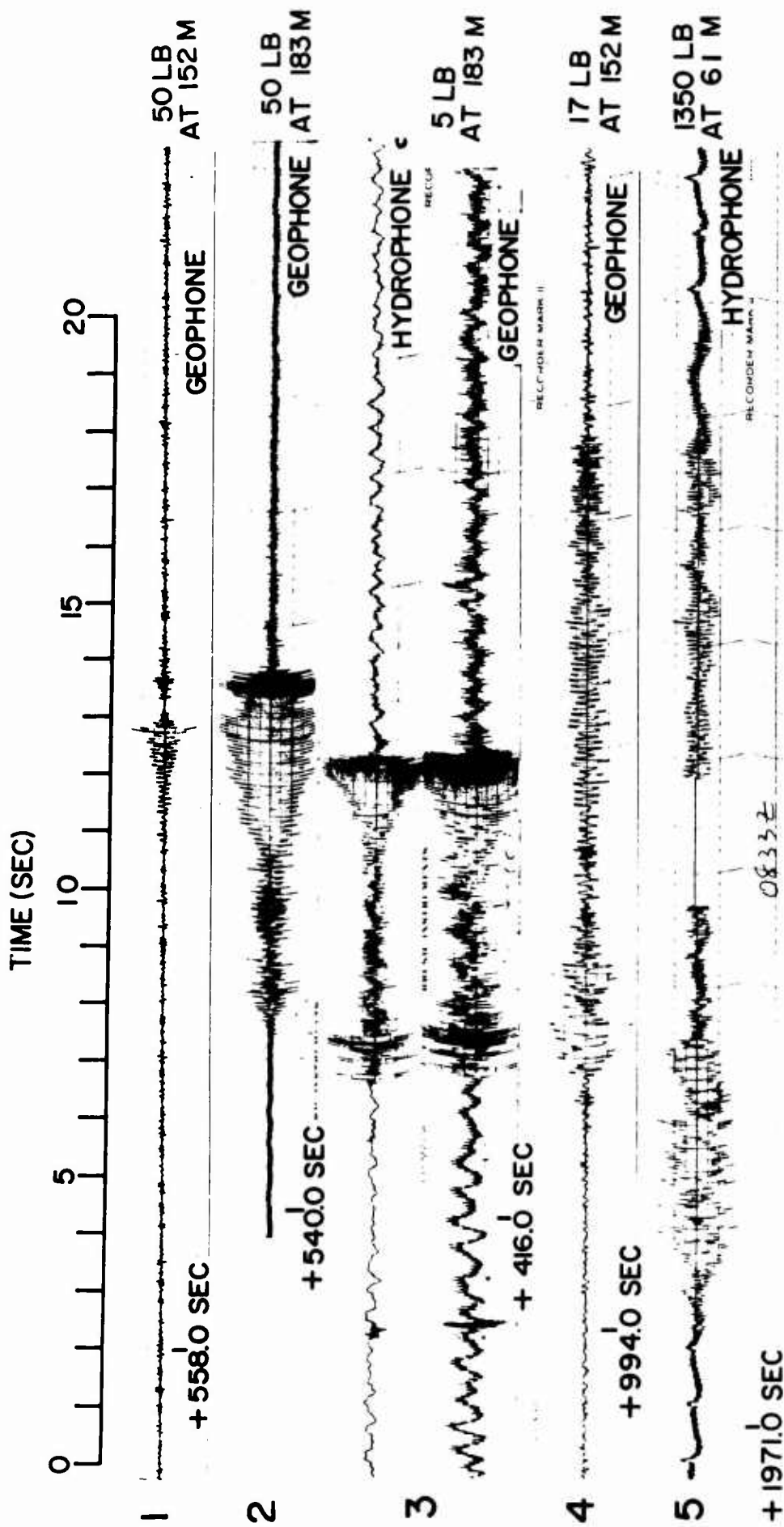
Fig. 5



● = LOCATIONS OF "NORTHWIND"
SHOTS RECORDED ON T-3'65



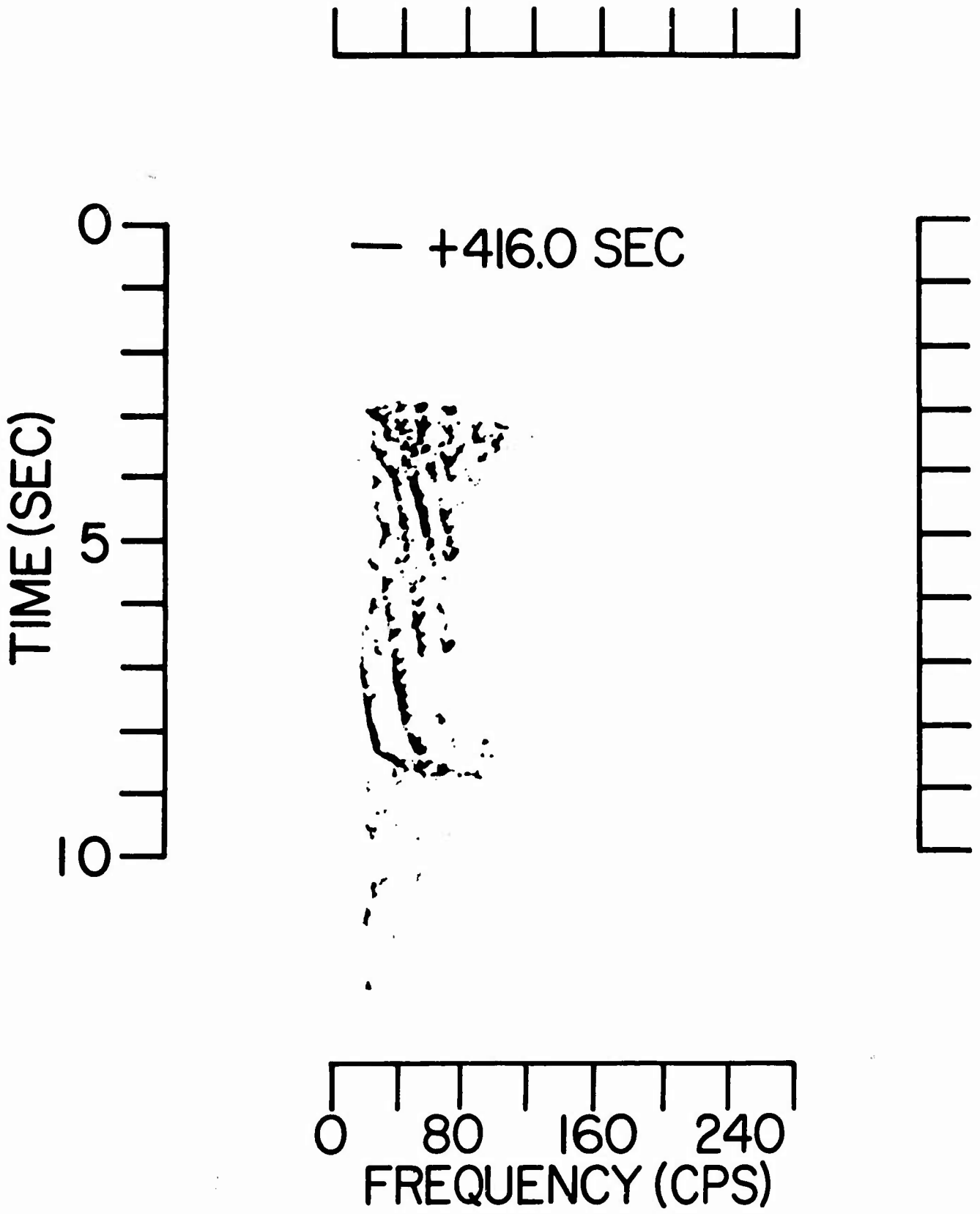
Fig. 6



sounds traveling along the various paths in Figure 2 (Kutschale, in preparation, a). It is these signals which are conveniently described in detail by normal mode theory.

Figure 5 shows the major bathymetric features of the central Arctic Ocean and the locations of drifting stations, Fletcher's Ice Island (T-3), Arlis II, Polar Pack I, and Charlie during experimental periods. Also shown in the figure are shot points occupied by the U. S. Coast Guard ice-breaker Northwind and Profiles 1 and 2 recorded on T-3 from small TNT charges dropped by a Navy aircraft. Over four hundred shots were recorded and analyzed. Ranges extend from one km up to 2860 km. The bottom topography is variable along paths 1 to 6, but along Profile 1 and part of Profile 2 the bottom was flat in the Canada Abyssal Plain. These transmission runs were made to measure the range dependence of the sound field without effects caused by changes in bottom topography. Figure 6 shows typical signals transmitted along paths 1 to 5 of Figure 5. The variation in amplitudes between the signals is principally caused by the variable bottom topography along the five profiles and the variable ranges to which the signals traveled. The signals transmitted along a deep-water path, such as path 3, begin with a sequence of sounds at arrival times in close agreement with those predicted by ray theory. Following these sounds a regular oscillatory wave train

Fig. 7



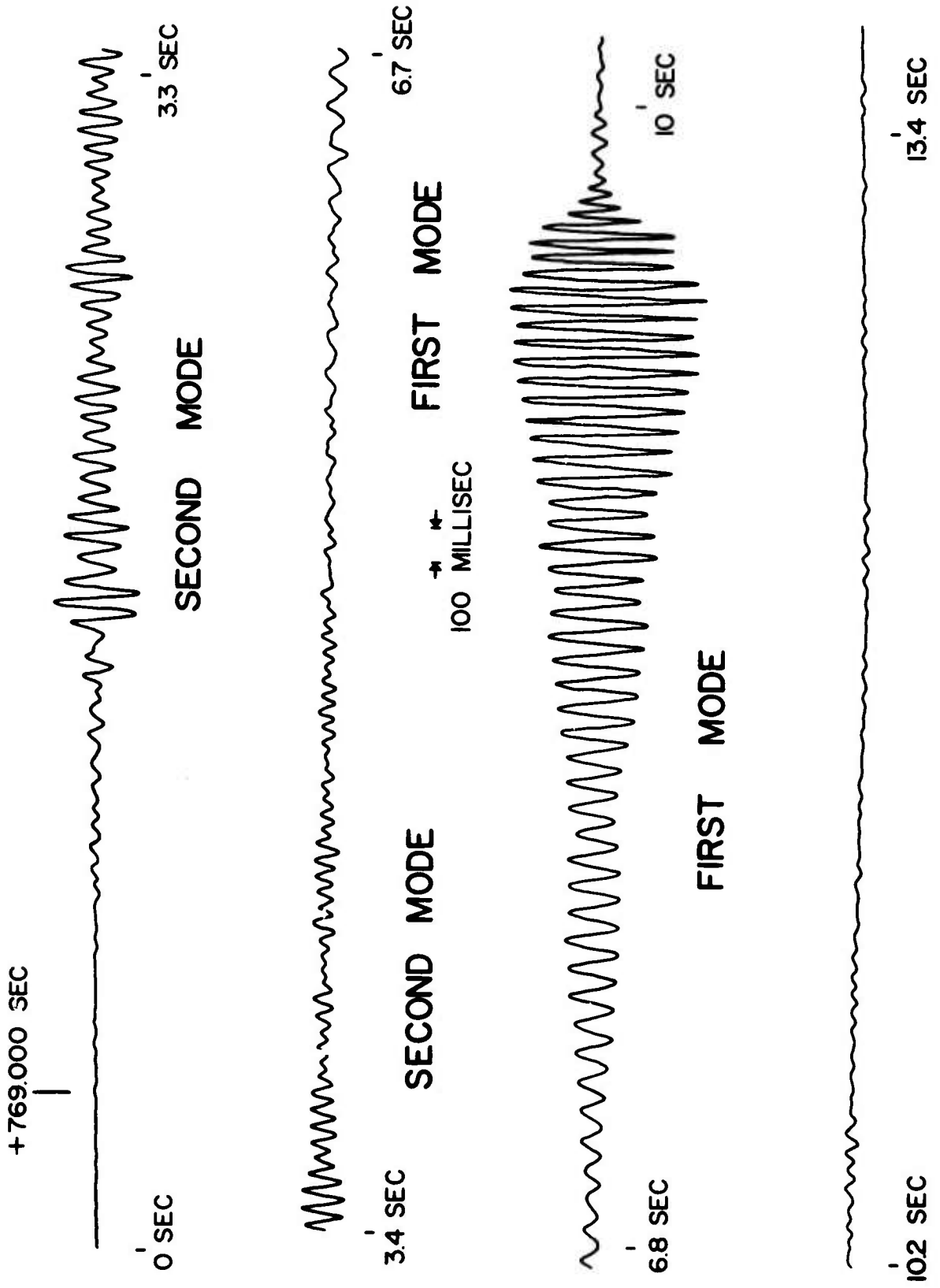


Fig. 8

is observed in which frequency increases with time. This wave train terminates with the last RSR sound and is followed by incoherent waves reflected from the ocean floor. The sound spectrogram of Figure 7 shows that the signals consist of a superposition of many normal modes of oscillation. Waves corresponding to each normal mode exhibit normal dispersion. At ranges greater than 1000 km only the first 2 or 3 normal modes are generally observed because of attenuation of waves corresponding to higher modes by the boundaries of the channel. The oscillogram of Figure 8 shows clearly the regular oscillatory appearance of waves corresponding to the first two normal modes.

The solution of the wave equation for the pressure or particle velocity perturbations generated by point sources in a layered medium makes possible a detailed comparison of observations with normal mode theory. The formulas for an n-layered, interbedded liquid-solid half-space bounded above by a rough layer are very complex (Kutschale, in preparation, b) and will not be given here. The solution for harmonic point sources is extended to explosive sources in the usual way (Pekeris 1948) and the Fourier integral for each mode is evaluated by the principle of stationary phase. The model of the underwater explosion at low frequencies and high frequencies for three bubble pulses is given by Weston (1960). Attenuation by the rough ice boundaries

Fig. 9

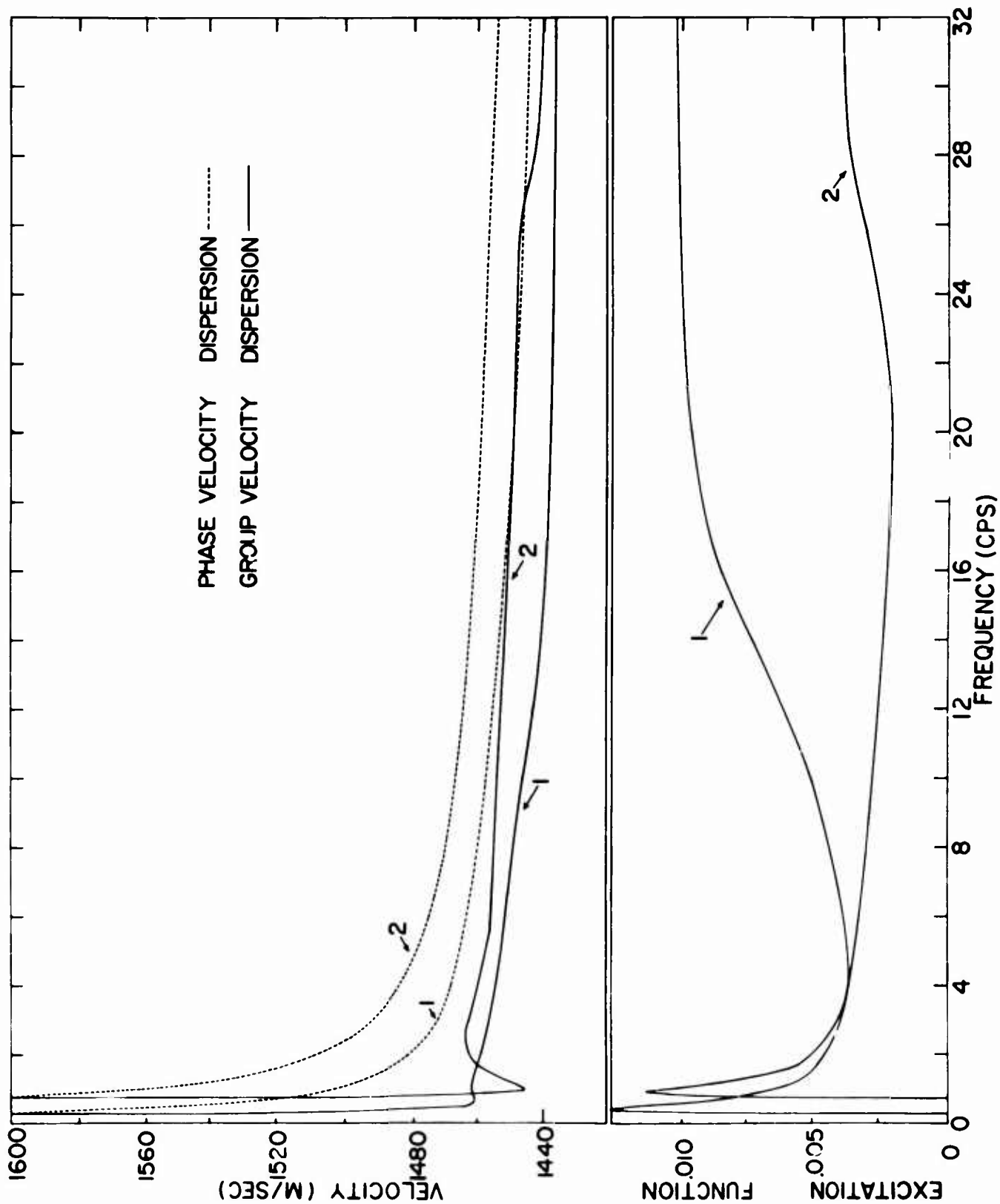


Fig. 10

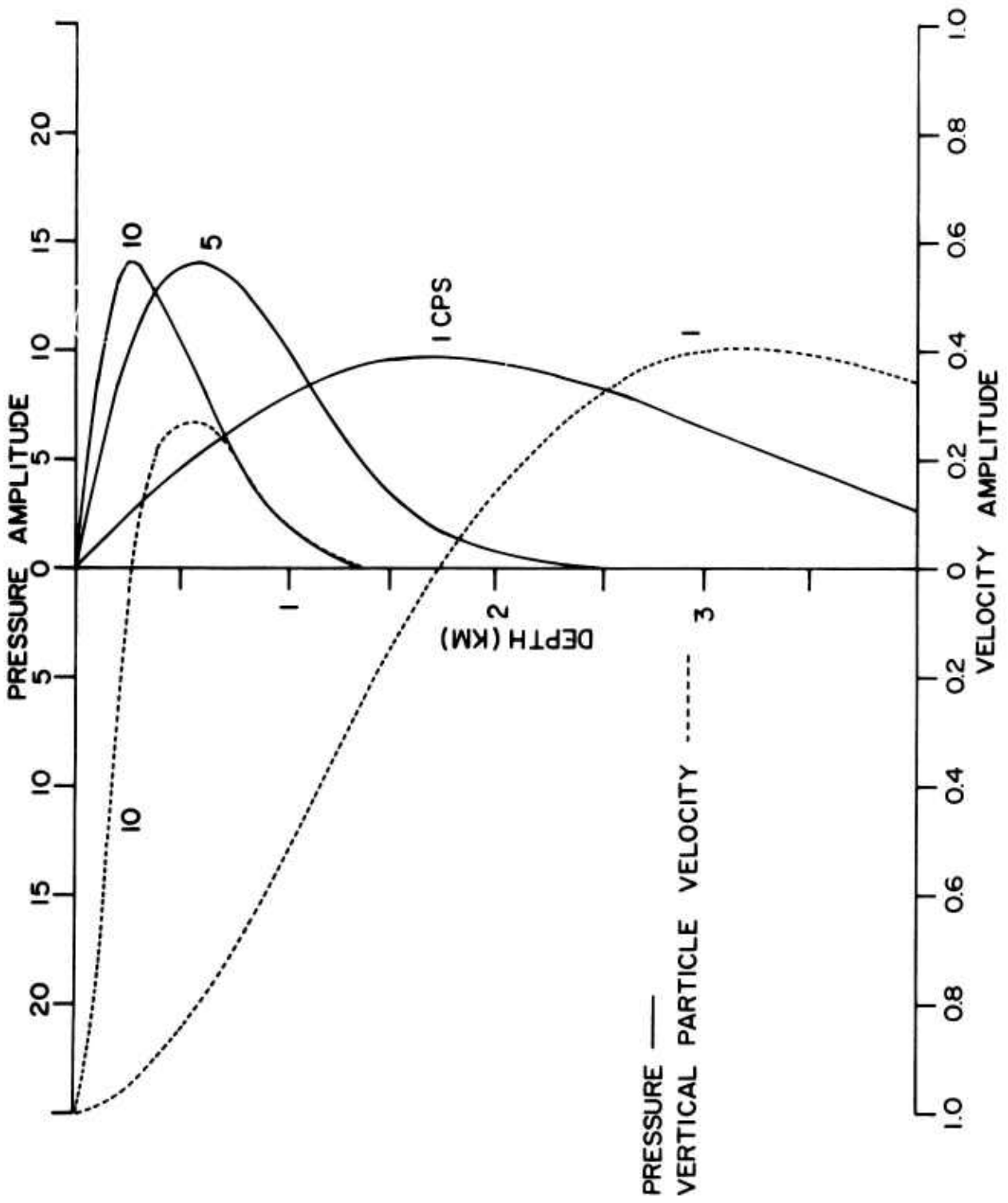
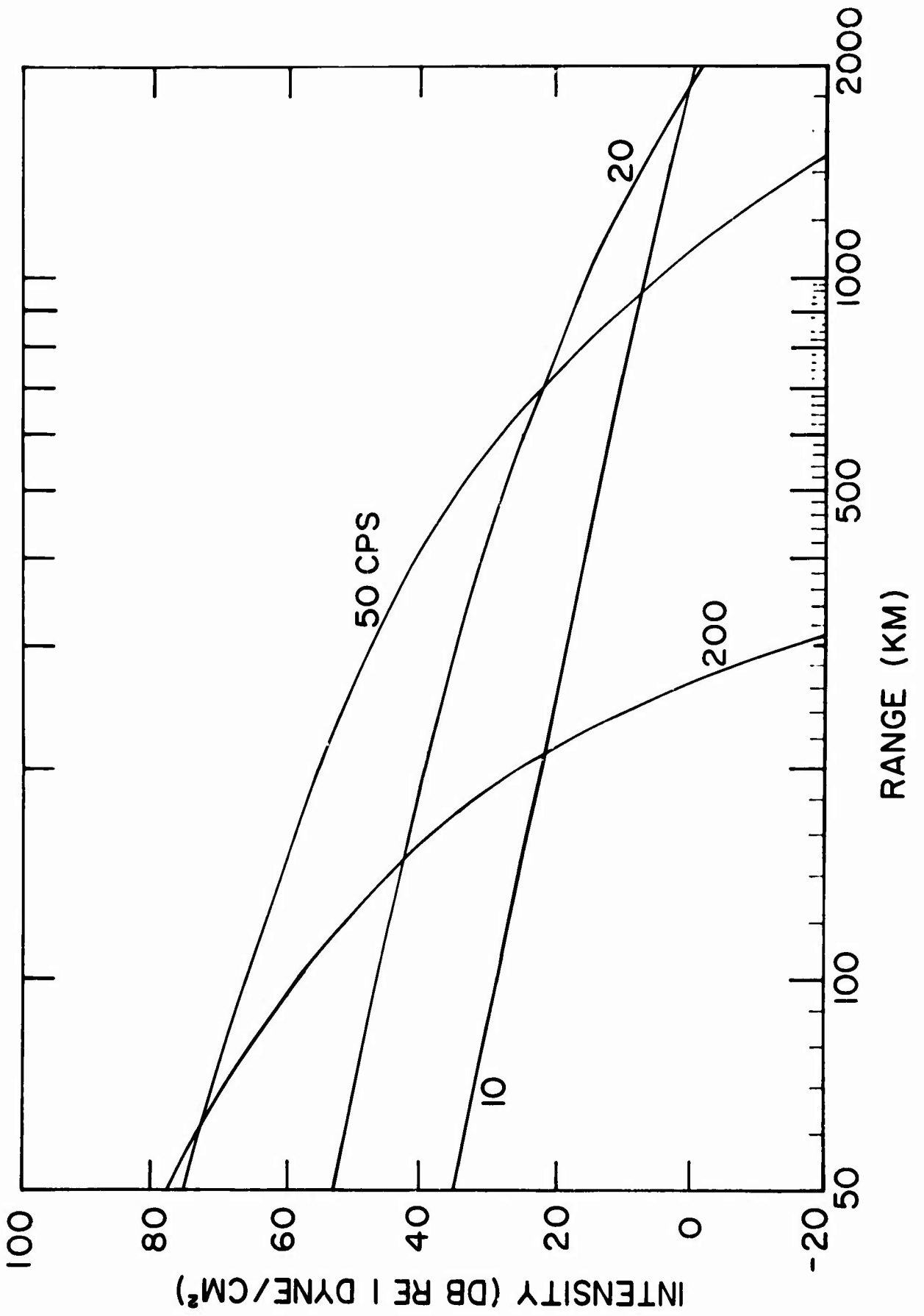


Fig. 11



is taken into account by multiplying the expression for pressure or particle velocity for each mode by an exponential term which is a function of the root-mean-square (rms) ice roughness below sea level, wave frequency, phase velocity dispersion, range for one cycle of a ray as a function of frequency, surface sound velocity, and the distance between source and detector. The solution of the wave equation in terms of normal modes is computed on the IBM 7094 or 360 digital computers in either single or double precision arithmetic.

We shall now present some computations for Model 2 and show that the normal mode theory for the layered models predicts quite reliably the frequency and amplitude characteristics of the observed acoustic signatures. Figure 9 shows phase- and group-velocity dispersion and the excitation function for the first two modes in the frequency range up to 32 cps. The excitation function is computed for the pressure solution of the wave equation for a harmonic pressure oscillation at the source. The attenuation by the ice boundaries is not included. The excitation function is a measure of wave amplitude which depends only on the layering of the medium. Figure 10 shows the dependence of pressure and vertical particle velocity on depth for the first mode at several frequencies. Figure 11 shows the range dependence of waves corresponding to the first mode when the surface is bounded by a rough ice layer. The amplitudes are computed in db re 1 dyne/

Fig. 12

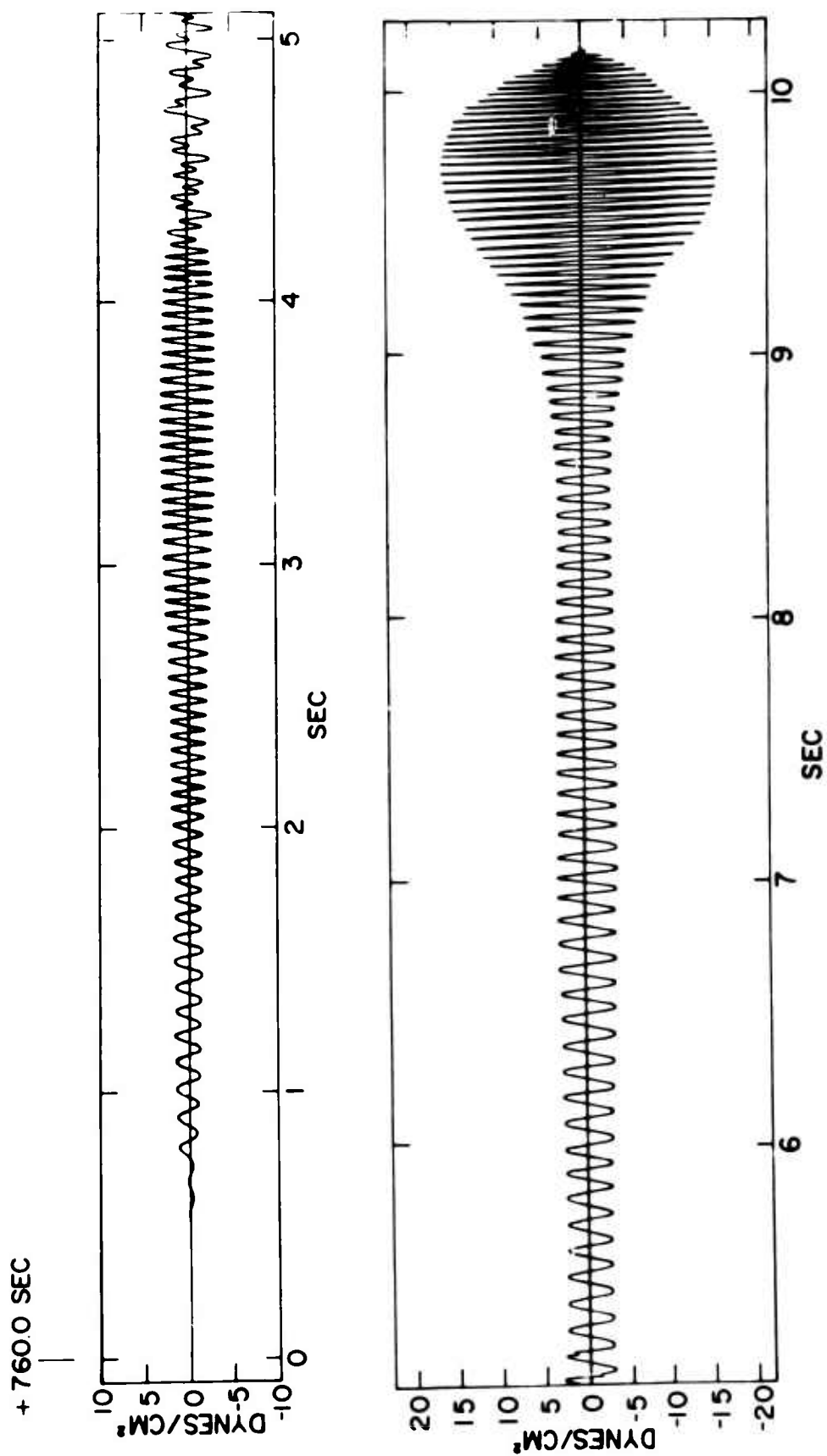
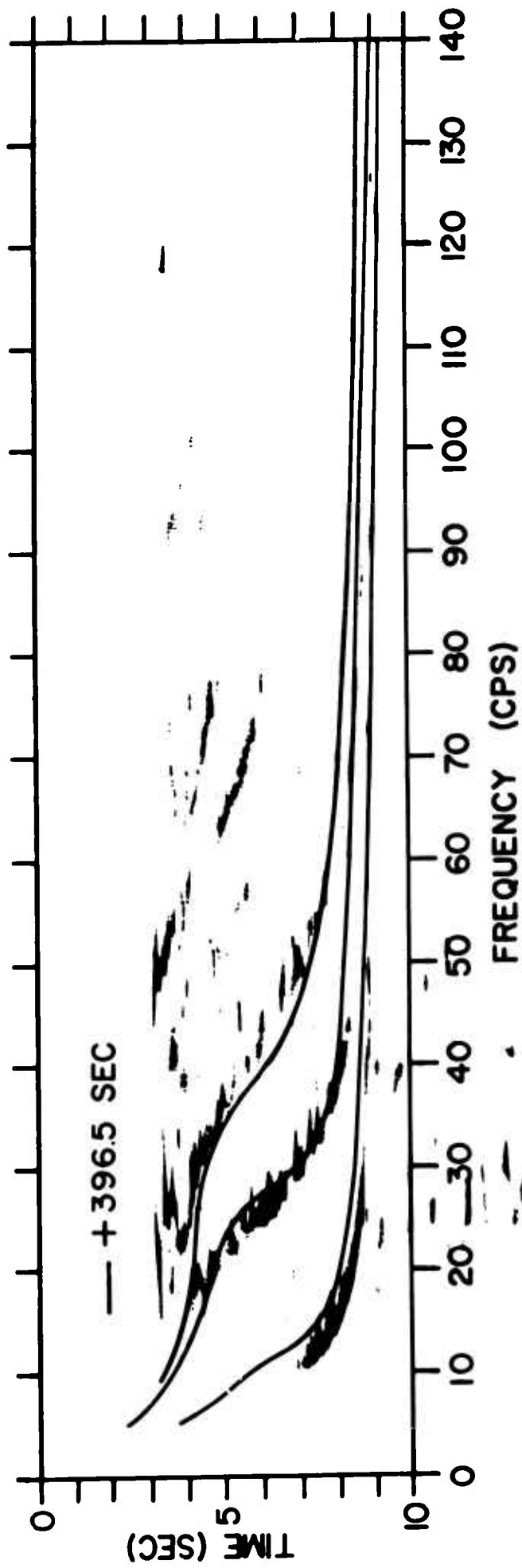


Fig. 13



cm^2 for a 5-lb charge of TNT at a depth of 150 m. The hydrophone is at a depth of 50 m. The rms ice roughness is 3 m. Curves of this type show that low-frequency waves will predominate at long ranges.

Figure 12 shows a computed oscillogram of pressure variations in dynes/cm^2 at the hydrophone for the same parameters used for computing the curves of Figure 11. Waves corresponding to the third and higher modes are neglected since they are weak at a range of 1106 km compared with waves corresponding to the first two modes. Although the oscillogram was computed for a charge about half as large as the one corresponding to the signal of Figure 8, the similarity of the two waveforms is nevertheless striking. Computations just completed specifically for the signal of Figure 8 are in close agreement with observation. These computations include the response of the listening system and the bathymetry along the propagation path.

In Figure 13 an observed sound spectrogram is compared with a computed one for a model similar to Model 2, but for a water depth of 2800 m. The signal traveled approximately along the deep-water path 3 of Figure 5. The agreement between theory and experiment is extremely good.

Fig. 14

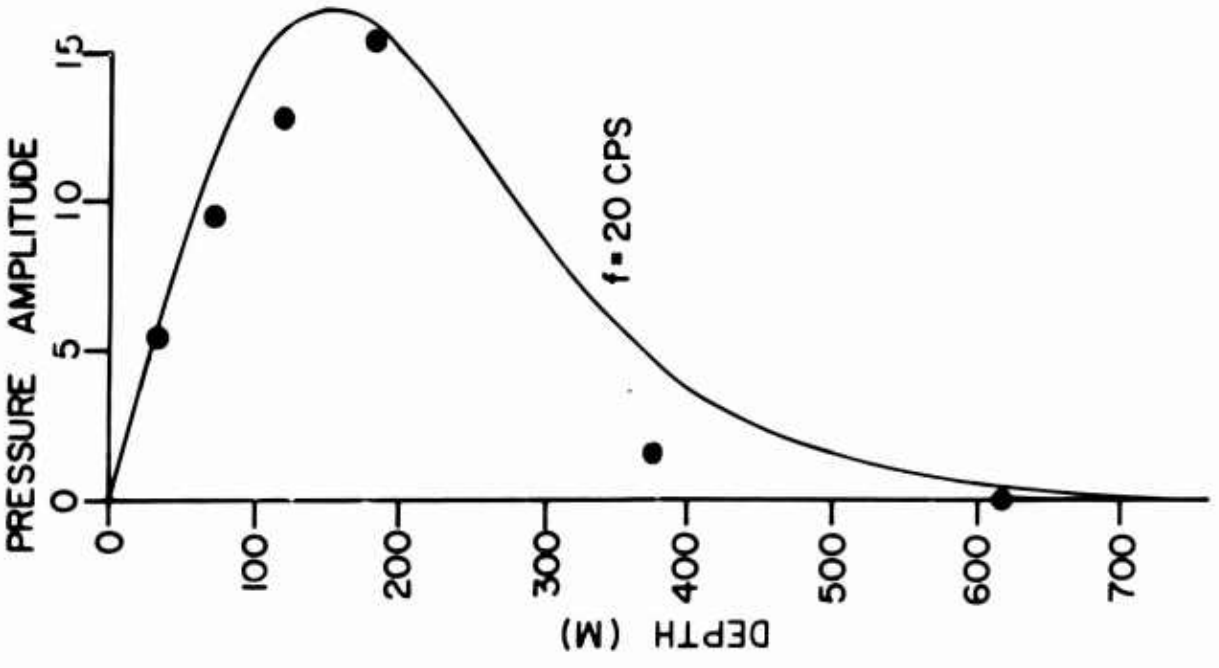
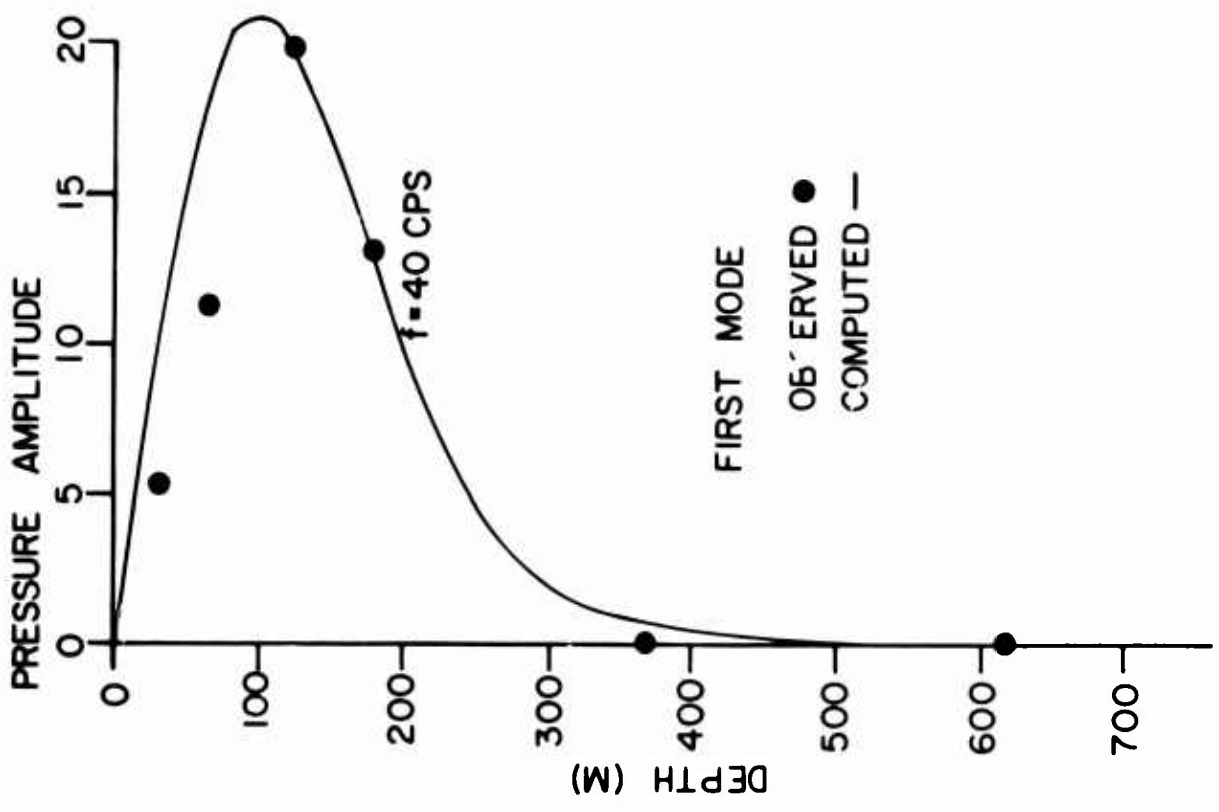


Fig. 15

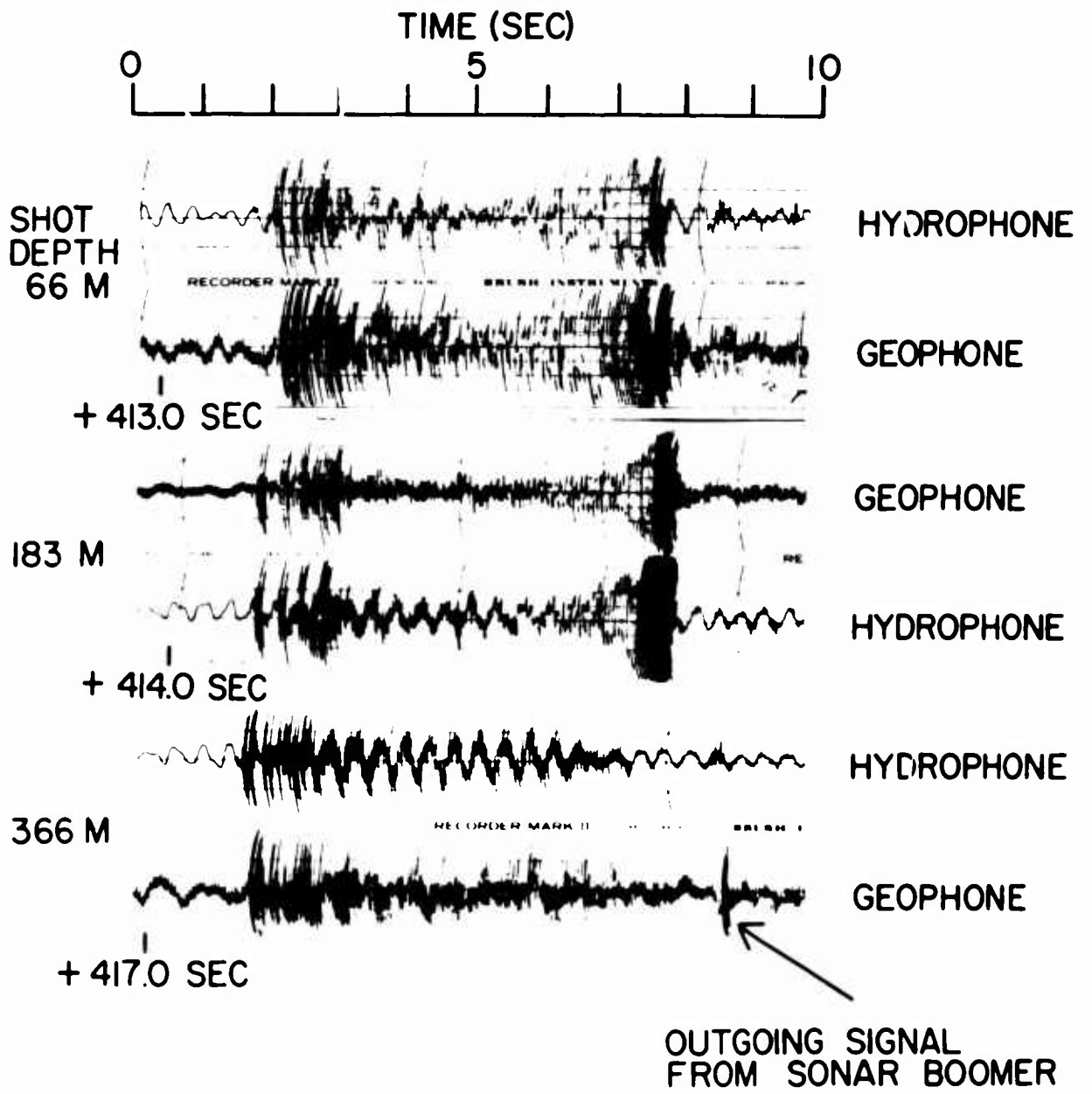


Fig. 16

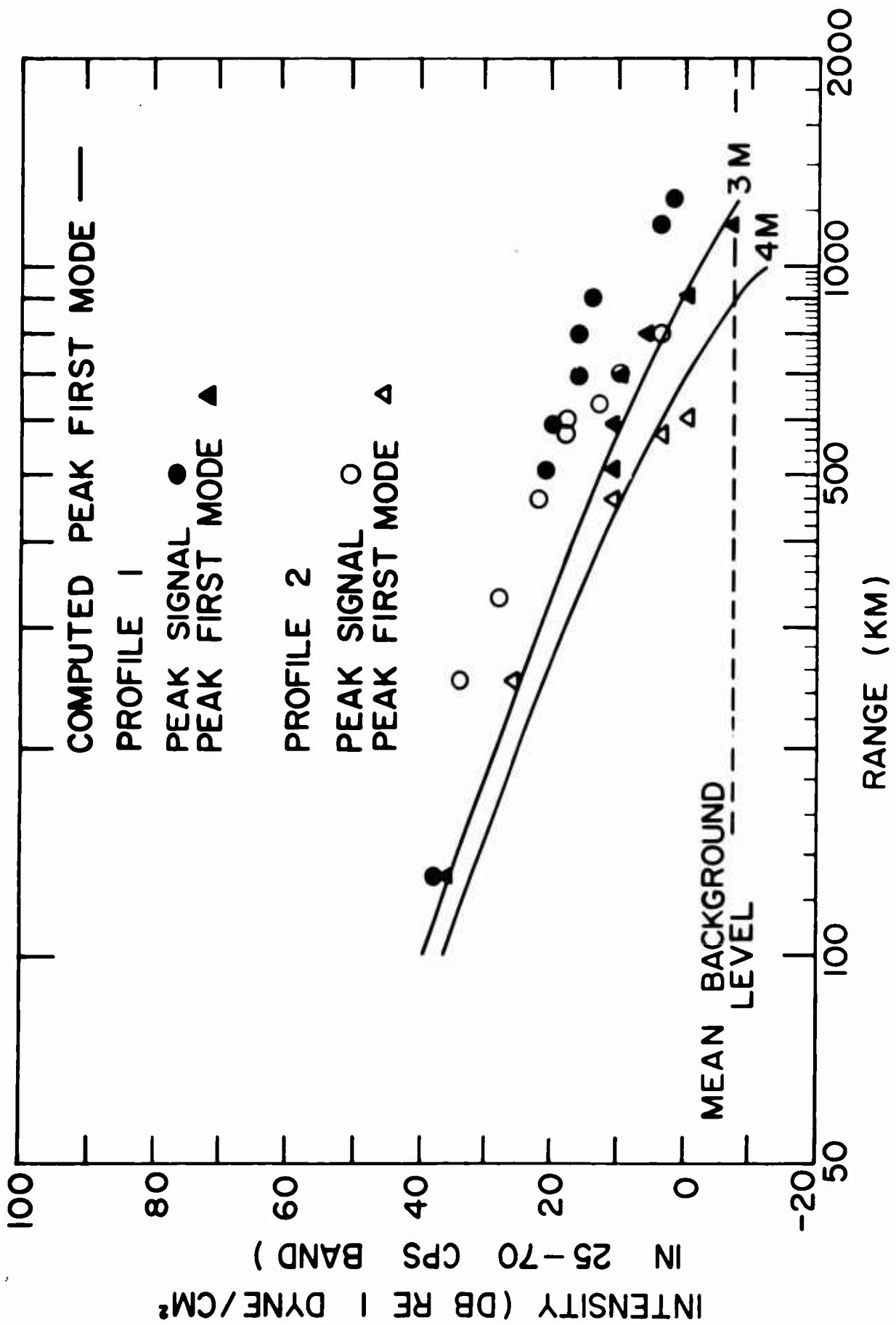
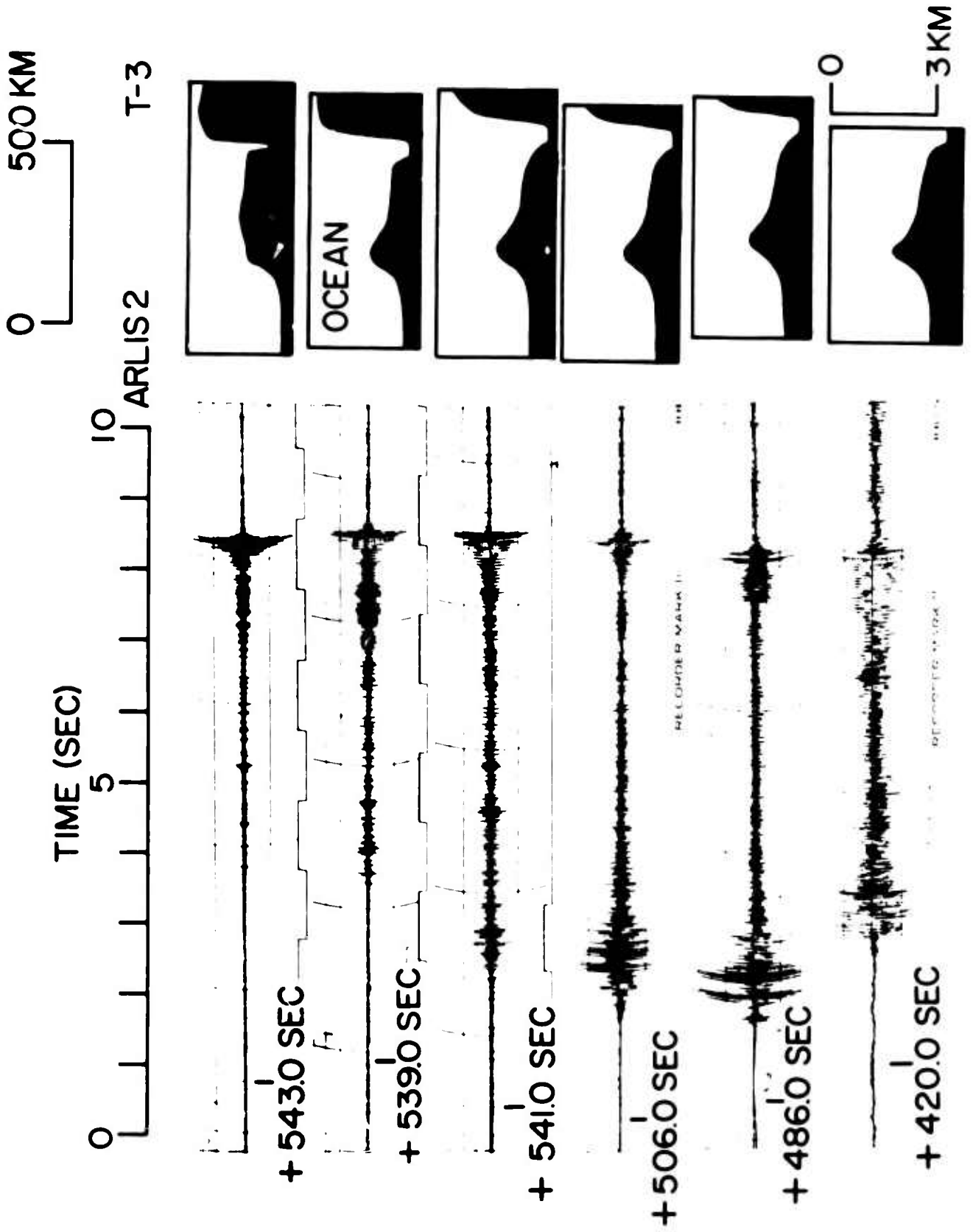


Figure 14 compares the measured and computed variation of pressure with depth for waves of the first mode at 20 and 40 cps. Some of the observed oscillograms are shown in Figure 15. The data shown in Figure 14 were corrected for the variation of the source spectrum of the 5-lb TNT charges with shot depth. The small disagreement between theory and experiment is probably due more to experimental errors of reading the oscillograms than to theory, since computations show that small variations in the sound velocity in the upper 400 m of water do not have a significant effect on the theoretical curves.

Figure 16 shows peak signal intensities and peak intensities of waves corresponding to the first normal mode in the band from 25 to 70 cps as a function of range along Profiles 1 and 2 of Figure 5. The more rapid decay of peak signal intensities along Profile 2 than along Profile 1 is probably due both to a rougher ice surface along Profile 2 and to the bottom topography on the Alpha Cordillera and continental margin. The peak signal intensity corresponds to the deep-penetrating RSR sounds which may have been weakened by reflection from the Cordillera and continental margin. On the other hand, the more rapid decay of waves of the first normal mode along Profile 2 than along Profile 1 is apparently due to the greater ice roughness along Profile 2. Figure 16

Fig. 17



shows computed peak signal intensities for the first normal mode in the band from 25 to 70 cps for an rms ice roughness of 3 and 4 m. The 3 m ice roughness fits the data from Profile 1 quite nicely, while at long ranges the 4 m ice roughness fits the data from Profile 2 reasonably well. The rms ice roughness of 3 to 4 m is in close agreement with the analysis by Mellen (1966) of Lyon's (1961) under-ice echograms made aboard a nuclear submarine.

Figure 17 shows the effect of bottom topography along the propagation path on the amplitudes of the signals. The sound sources were 1-lb TNT charges fired at a depth of 71 m. The hydrophone was at a depth of 46 m. The propagation paths lay between paths 2 and 3 of Figure 1. This experiment shows that the first strong sound corresponds to an RSR ray which has passed over all bottom topography without suffering a bottom reflection. For this sequence of shots, the shallowest point along the paths is about 350 m. This corresponds to a speed of sound or phase velocity of 1454 m/sec, and to a group velocity or mean horizontal velocity of 1445 m/sec, which is in good agreement with the measurements.

In shallow water, sounds may be propagated to moderately long ranges by repeated reflections from the surface and bottom (Hunkins and Kutschale 1966). The propagation is not as efficient as in deep water

Fig. 18

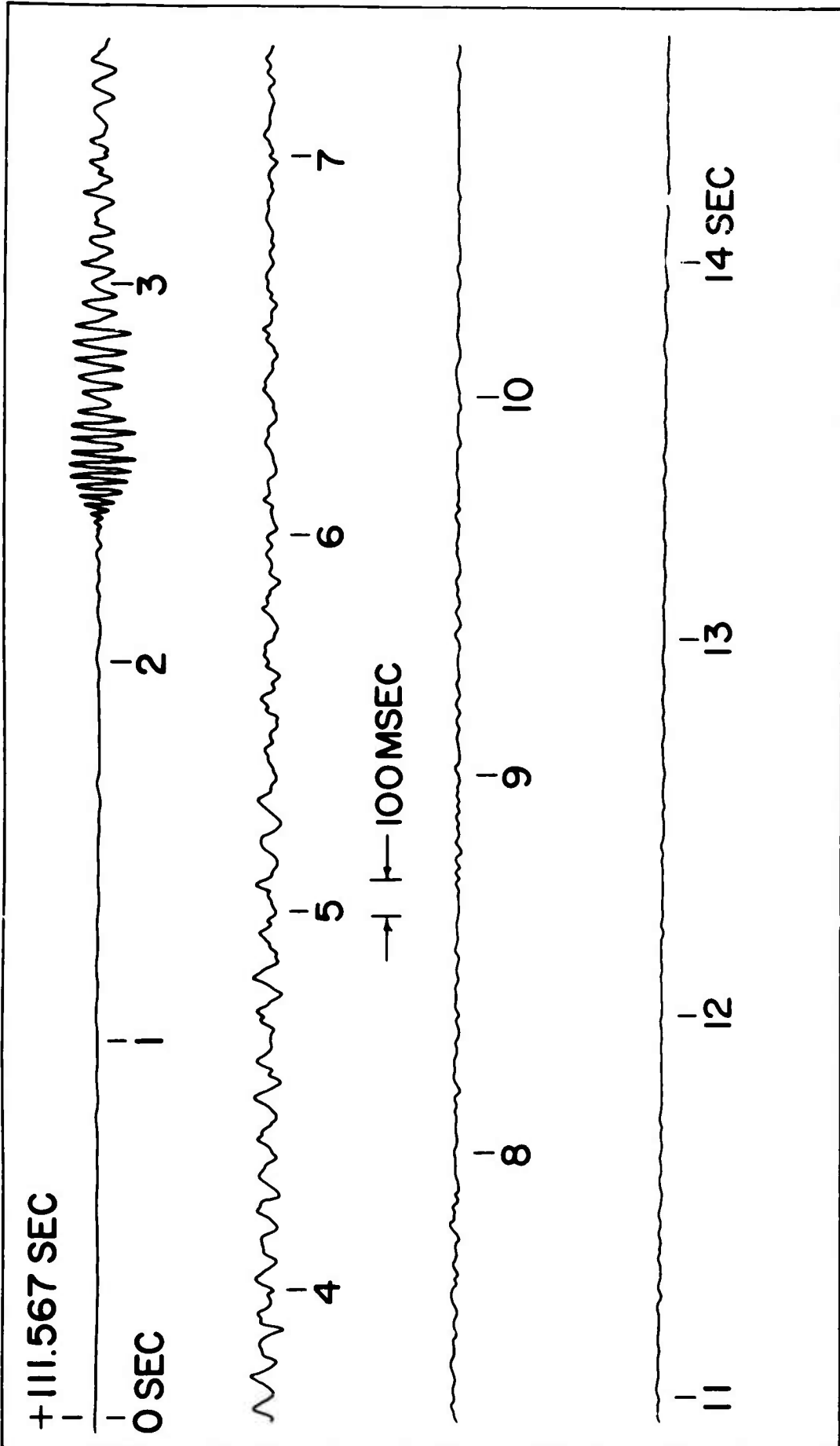


Fig. 19

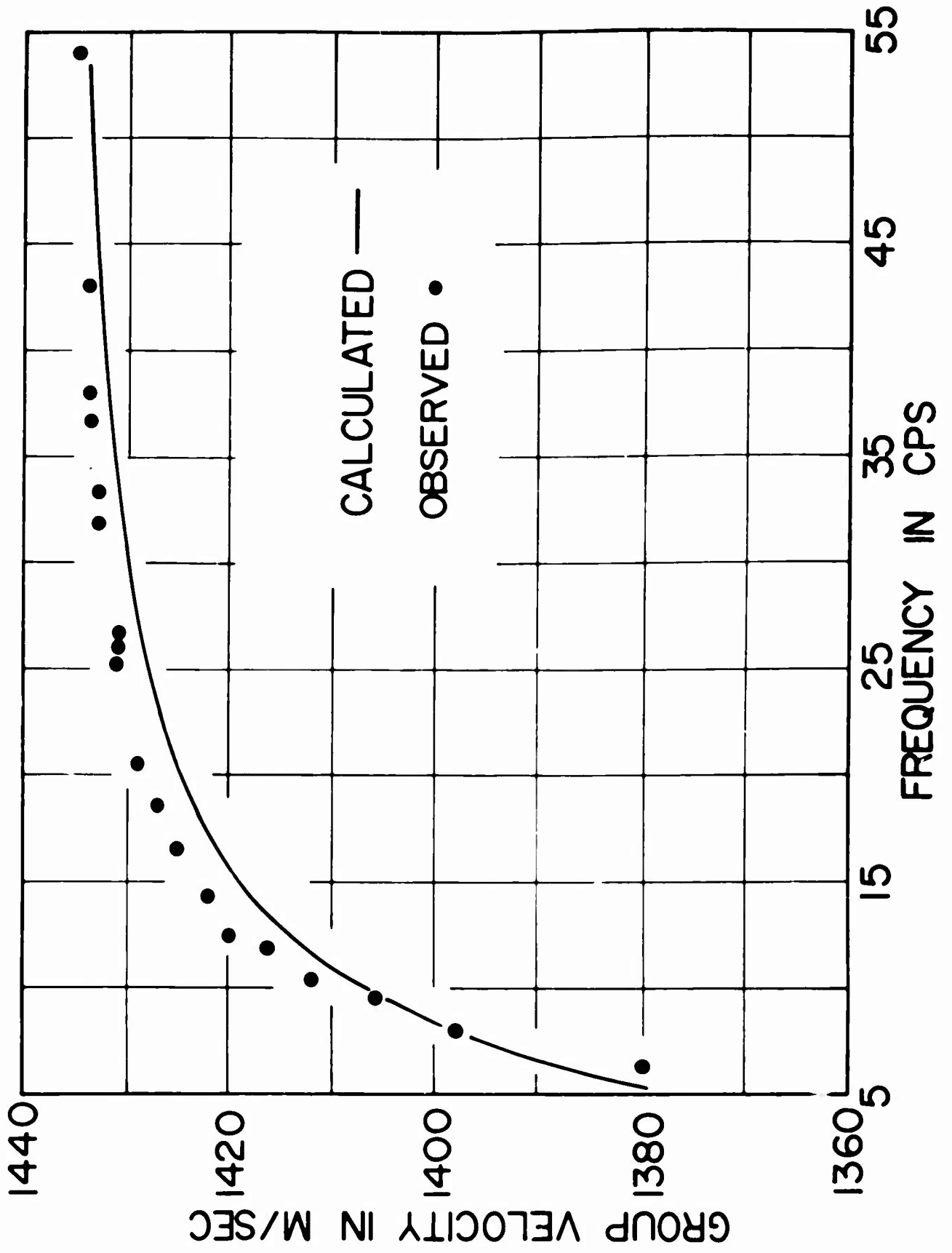
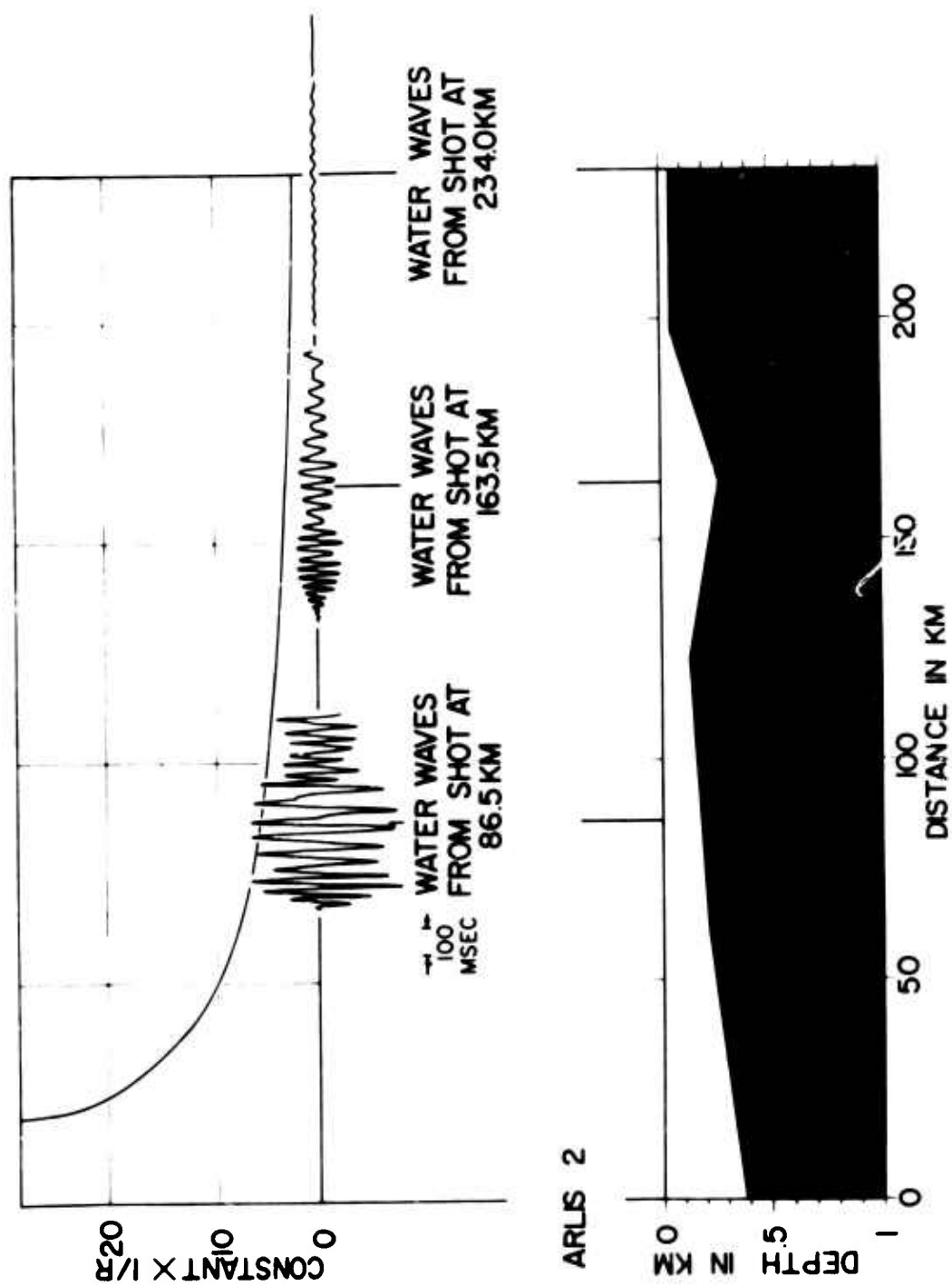


Fig. 20



because of the absorption of sound in the sediments and scattering of sound from the ocean bottom. The propagation is generally quite variable depending on the water depth and the nature of the bottom. Figure 18 shows the water waves from a 1100-lb TNT charge, exploded at a depth of 16 m recorded aboard ARLIS II at a range of 163.5 km. Notice the inverse dispersion of the first normal mode in contrast to the normal dispersion observed in the deep ocean. Figure 19 shows that this dispersion is in good agreement with that computed for the layered model given in Table 2. Figure 20 shows diagrammatically the decrease of peak amplitude with range for three shots recorded on ARLIS II. The amplitudes have been normalized to a 800-lb TNT charge. The peak amplitude, which corresponds to a frequency of 18 cps, decreases as the -1.85 power of range in the range interval from 75 to 275 km rather than the inverse first power of range at this frequency and in this range interval observed in deep water. Signals from large charges fired in shallow water have been recorded aboard listening stations in deep water, and also for the reverse situation. In these cases when the length of the shallow-water path is a sizable fraction of the deep-water path, computations are made for each segment of the path separately and they are then combined for the total path.

Table 2. Parameters for Computing Shallow Water Dispersion.

Layer	Longitudinal Velocity km/sec	Transverse Velocity km/sec	Density gm/cm ³	Layer Thickness m
1	1.435	-	1.025	230
2	1.75	-	1.6	200
3	2.7	-	2.08	00

Background Noise

An important acoustical parameter of the ocean is the natural background noise. It does not affect sound propagation, but it is extremely important to all aspects of signal detection and processing. An important problem is to isolate the principal sources of noise, measure their strengths, and determine how the noise is propagated away from the sources. Measurements over long periods of time at many locations are necessary to determine dependence of the noise on time, location, and direction.

The principal source of noise in the Arctic Ocean is the ice cover. This ice is in continual motion under the influence of wind and currents and thousands of tons of ice may be displaced vertically and horizontally when a large pressure ridge is formed or a floe breaks up. The air-borne sounds generated by this ice movement are often heard by ear up to a km from the active area. The sound is commonly a low-frequency rumble. Ice vibrations may also be felt under foot if one is standing on the floe which is breaking up or where a pressure ridge is being formed. Besides these large-scale ice movements, the ice may be under sufficient stress to induce small ice quakes. This is particularly common when the ice is under thermal stress during periods of rapid temperature drop in the spring and fall. The air waves generated by these ice quakes have a snapping sound and their frequency of occurrence may be over one per second. Other sources of noise

which may be heard by ear at times are wind-blown snow moving over the ice and gravity waves splashing in open leads.

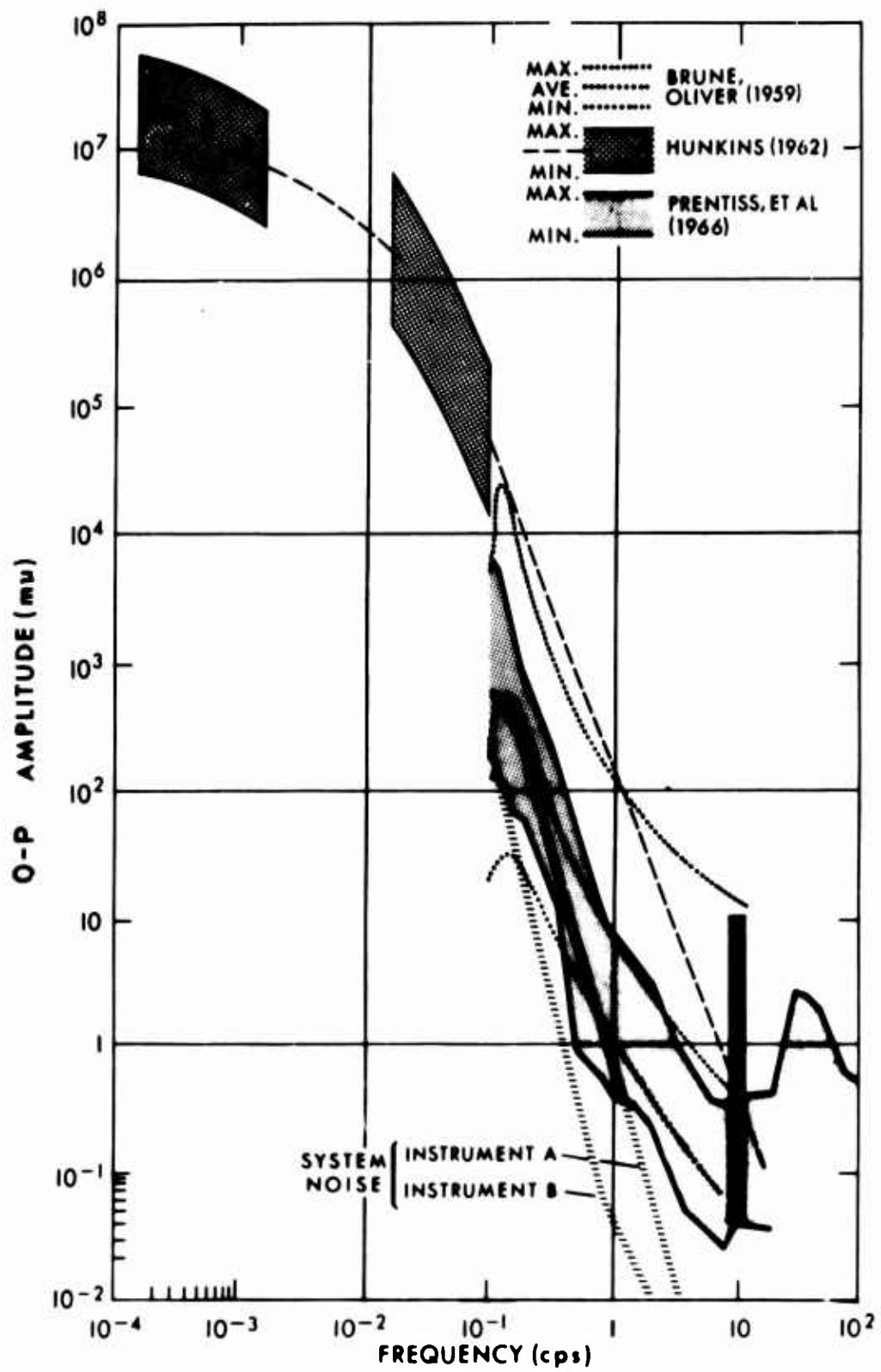
The natural background noise on the ice and at depth is quite variable in strength. This is to be expected since the noise level depends largely on the relative motion of the pack ice in the immediate area under investigation, and this motion may be from practically zero when all floes are moving with a uniform velocity to highly variable velocities of neighboring floes during breakup and pressure ridging. The strength of the background noise does not always correlate with the local wind speed, but there is a higher probability of high noise levels during storms than during periods of prolonged calm. The noise may also have a directional character, depending on the locations of the principal ice activity. When local ice activity is low and the noise level is correspondingly low, sounds may arrive from considerable distances traveling in the sound channel. Under these conditions the noise level falls off rapidly with increasing frequency because of attenuation of the high-frequency waves by scattering.

The background noise on the ice and at depth in the ocean is measured by single detectors and vertical and horizontal arrays of detectors. Recordings from a single detector made over long periods of time yield information on the time variation of the noise. Recordings from arrays provide information on the direc-

tional properties of the noise and permit an identification of the types of waves present in the noise. Hydrophones at depth pick up sounds traveling along paths like those of Figure 2. On a typical day, the scraping and grinding of ice is heard on a loud speaker interrupted occasionally by explosion-like sounds from ice quakes. At night in the spring and fall thermal cracking may be so strong and frequent that noise from other sources above 20 cps is blocked out. The hissing sound of wind-driven snow is heard during storms in the cold months and during the warm months sounds from marine mammals are sometimes heard. On a very quiet day, even the splashing of waves in a nearby lead may be heard.

Noise levels in the water generally build up and decay over periods of at least a day, but the ice vibrations may fluctuate by more than 40 db over periods of less than one hour. The water-borne sounds come from many active floes, while the strong ice vibrations are generally confined to the floe on which the seismometer is located. The dominant ice vibrations correspond to flexural waves generated by ice movement at the boundaries of the floe and as this movement increases in magnitude and then weakens so do the flexural waves. The flexural waves are surface waves traveling in the ice sheet and, therefore, pressure perturbations decay exponentially with depth. Only seismometers on the ice and

Fig. 21



hydrophones directly beneath the ice detect these waves. The flexural waves are identified by their characteristic inverse dispersion and by the particle motion of the waves. When the movements at the boundaries of the floe are small, then the principal source of noise may be sound transmitted through the water from other active floes, either near or distant. Figure 21 shows vertical particle motion measured in octave bands from data taken on ARLIS II (Prentiss et al., 1966). For comparison, the curves of Brune and Oliver (1959) for land noise and Munkins (1962) for the Arctic Ocean are shown in the figure. The noise curves of Prentiss et al. are for average levels, not for bursts of noise occurring during particularly active times. Even so, the variation of noise levels is more than 30 db, corresponding to levels from below quiet land sites up to noisy land sites.

REFERENCES

- Alberta Society of Petroleum Geologists Geological Map of the Arctic, 1960. University of Toronto Press, Toronto.
- Brune, J. N., and J. Oliver, 1959. The seismic noise of the earth's surface. Bull. Seismol. Soc. Am., 49, pp. 349-353.
- Ewing, M., and J. L. Worzel, 1948. Long-range sound transmission in Propagation of Sound in the Ocean. Geol. Soc. Am. Mem. 27, pp. 1-35.
- Hunkins, K., 1962. Waves on the Arctic Ocean, J. Geophys. Res., 67, pp. 2477-2489.
- Hunkins, K., and H. Kutschale, 1963. Shallow-water propagation in the Arctic Ocean. J. Acoust. Soc. Am., 35, pp. 542-551.
- Kutschale, H. The phase integral method applied to long-range sound propagation in the Arctic Ocean, in preparation, a.
- Kutschale, H. Surface waves from sources at depth in a multi-layered liquid-solid half-space with numerical computations for CW and pulse propagation in the Arctic SOFAR Channel, in preparation, b.
- Lyon, W. K., 1961. Ocean and sea ice research in the Arctic Ocean via submarine. Trans. N.Y. Acad. Sci., 23, pp. 662-674.
- Mellen, R. H., 1966. Underwater acoustic scattering from Arctic ice. J. Acoust. Soc. Am., 40, pp. 1200-1202.
- Pekeris, C. L., 1948. Theory of propagation of sound in the ocean. Geol. Soc. Am. Mem. 27, pp. 1-117.

Prentiss, D., E. Davis, and H. Kutschale, 1966. Spectral character of ice vibrations in the Central Arctic Ocean from 0.1 to 100 cps. J. Acoust. Soc. Am., 40 (abstract), p. 1279.

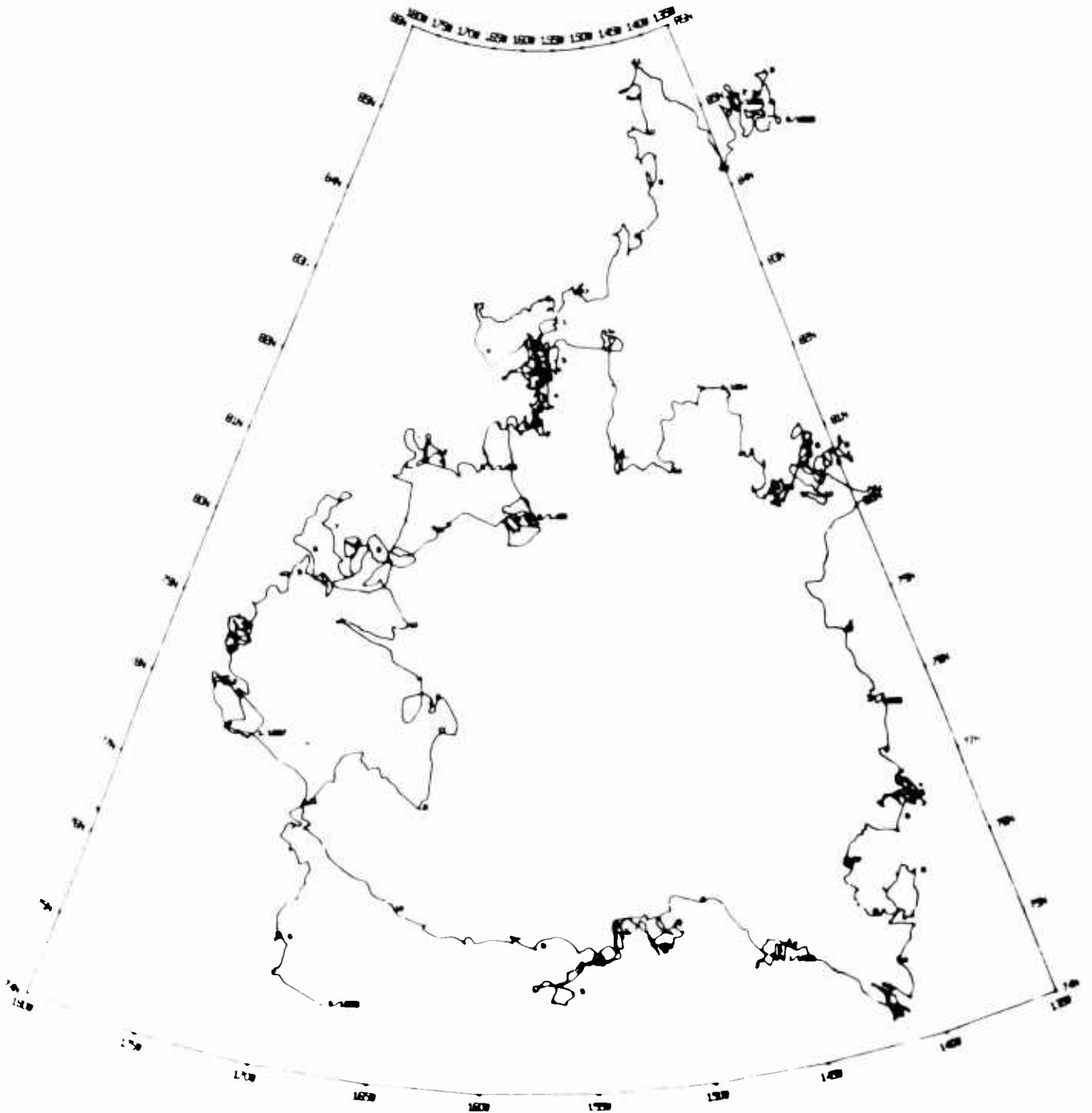
CAPTIONS FOR FIGURES

- Fig. 1 Models representing the Arctic sound-velocity profile.
- Fig. 2 Ray paths for model 1 of Figure 1. Source depth 100 m.
- Fig. 3 Mean horizontal velocity and range per cycle for Model 1 of Figure 1.
- Fig. 4 Time sequence of arrivals for Model 1. Surface source. Surface detector.
- Fig. 5 Bathymetric map of the central Arctic Ocean. Propagation paths are numbered 1 to 6. Transmission profiles 1 and 2 recorded on Fletcher's Ice Island (T-3) during May 1968. Contours based on Geologic Map of the Arctic (1960).
- Fig. 6 Typical signals transmitted along paths 1 to 5 of Figure 5.
- Fig. 7 Sound spectrogram of 5-lb TNT charge fired at a depth of 122 m. Hydrophone at a depth of 46 m. Waves traveled a distance of 609.4 km along path 3 of Figure 5.
- Fig. 8 Oscillogram of signal transmitted along path 6 of Figure 5. Range 1118.2 km. 9-lb TNT fired at a depth of 152 m. Hydrophone at a depth of 61 m. Passband of listening system 10-21 cps.
- Fig. 9 Phase- and group-dispersion for first two models computed for Model 2. Excitation function for first two modes for Model 2.

- Fig. 10 Variation of pressure and vertical particle velocity with depth for the first mode at several frequencies. Computations for Model 2.
- Fig. 11 Range dependence of waves of the first normal mode. Computations for Model 2 with 3 m root-mean-square (rms) ice roughness. 5-lb TNT charge at 150 m. Hydrophone at 50 m.
- Fig. 12 Computed oscillogram of pressure variations for Model 2. Ice roughness 3 m (rms). 5-lb TNT at 150 m. Hydrophone at 50 m. Range 1106.0 km.
- Fig. 13 Comparison of observed and computed dispersion for first three modes. Computations for model similar to Model 2 but with a water depth of 2800 m.
- Fig. 14 Comparison of observed and computed variation of pressure with depth at 20 and 40 cps. Computations for model similar to Model 2 but with a water depth of 2800 m.
- Fig. 15 Four oscillograms which provided some of the data of Figure 14. Shots 5-lb TNT. Signals traveled about 600 km approximately along path 3 of Figure 5.
- Fig. 16 Peak signal intensities and peak intensities of waves corresponding to the first normal mode as a function of range. Computations for Model 2 with ice roughnesses of 3 m and 4 m. Shots 1.8-lb TNT at 274 m. Hydrophone at 30 m.

- Fig. 17 Oscillograms showing effect of bottom topography on the amplitudes of the waves. Shots 1-lb TNT at a depth of 71 m. Hydrophone at 46 m. Propagation paths between paths 2 and 3 of Figure 5.
- Fig. 18 Water waves from 1100-lb TNT charge fired at a depth of 16 m. Distance 163.5 km. Average water depth about 230 m. Waves of first mode predominate.
- Fig. 19 Observed dispersion of waves of the first mode from several shots compared with first mode computed for model given in Table 1.
- Fig. 20 Water-wave transmission loss and bathymetric profile for shots recorded on ARLIS II.
- Fig. 21 Ambient ice vibrations recorded on ARLIS II analyzed in octave bands. For comparison, Brune and Oliver (1959), and Hunkins (1962) curves shown. System B was used to record during low noise levels.

Fig. 22



INTERPOLATED DRIFT TRACK - FLETCHER'S ICE ISLAND (7-3)
MAY 1962 TO JUNE 1969

Geophysical Investigations from Fletcher's Ice Island

I. Navigation

The drift track for T-3 for the period May 14, 1962 to June 12, 1969 is shown in Figure 22. The track is based upon approximately 2100 celestial positions, and over 7000 satellite derived fixes. Prior to April 14, 1967, when the AN/SRN-9 Radio Navigation Set became operational, positions were fixed with a Wild T-2 theodolite, whenever weather permitted. For the periods between fixes, observations of wind speed and direction were used to determine the most probable drift. Nansen observed from the drift of the Fram that the ice drift was approximately $1/50$ the wind speed in a direction $28-30^{\circ}$ to the right of the wind (in the Northern hemisphere). A computer program was written to solve for the ice motion between fixes based on a similar assumption, except that the speed factors and deviation angles are computed and used in the calculation of interpolated positions. In the event that the computed speed factor exceeds 0.035 (75% above Nansen's average value) or falls below 0.0075 (37% of Nansen's value), the motion is ascribed to both wind drift (using Nansen's average parameters) and to a steady current, whose velocity is determined. This occurs when currents or the effects of winds at a distance cause small movements during periods of calm.

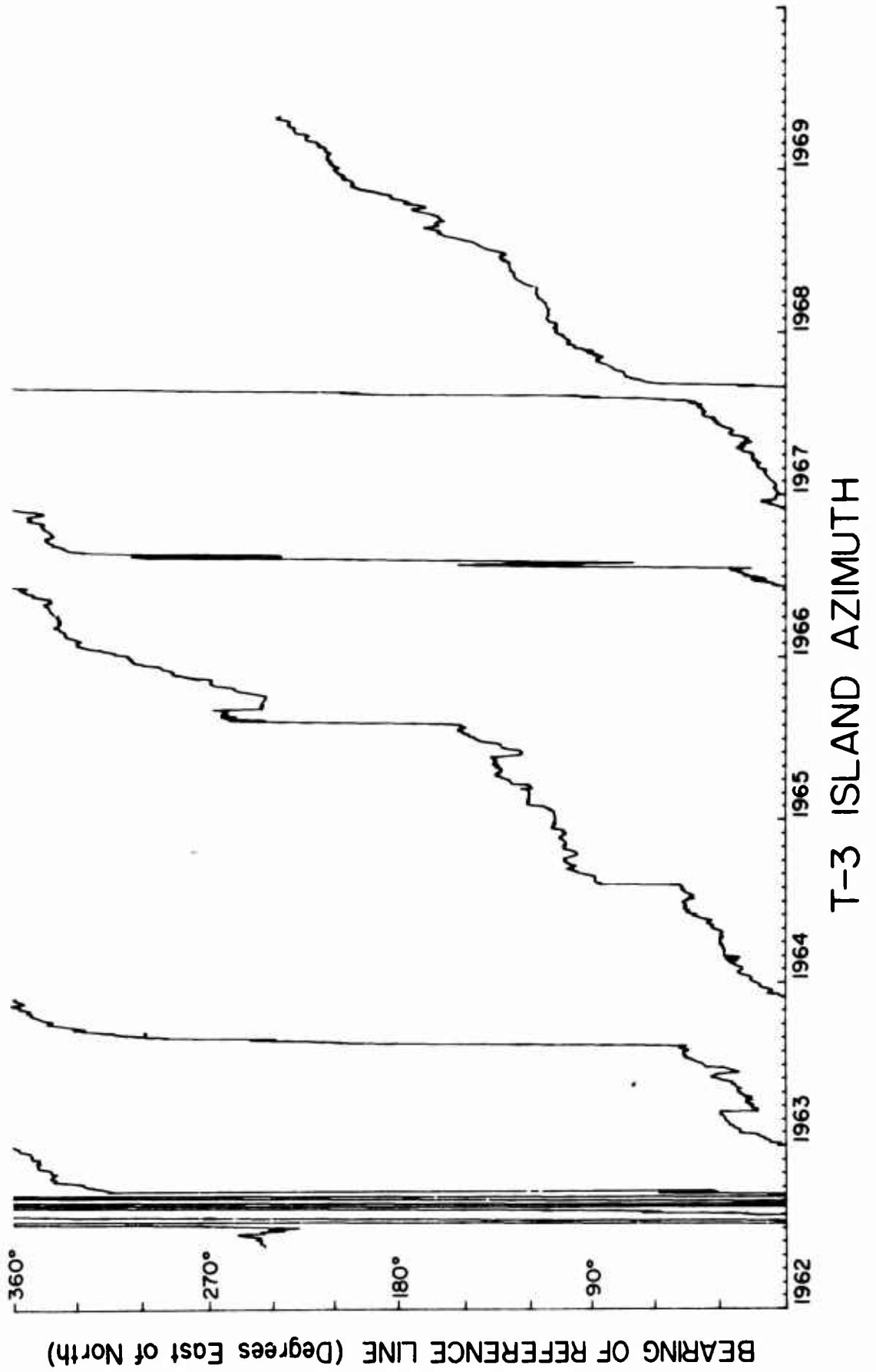
When satellite observations became available, the navigation problem became one of too much data or too little. During waking hours many passes were tracked, but no data were obtained during the "night" or during periods of equipment malfunction. During long periods with no data, celestial observations were again taken, and during the "nightly" gaps, wind drift interpolations were used. This treatment resulted in approximately 22,000 positions for the period. These were then plotted as north-south and east-west components as a function of time, and any sharp changes in position were investigated and corrected. The data were then interpolated to hourly intervals, and filtered with a variable length cosine window filter in order to remove any sharp peaks and random errors in the closely packed satellite data. The resulting track, plotted at two-hour intervals, is shown in the figure.

The celestial observations were processed by computer in an attempt to increase accuracy, achieve uniformity of computation, and remove myriad human errors. Two programs were written to compute the Greenwich hour angle, declination, semi-diameter, and horizontal parallax of the sun and stars (Program EDOC), or the moon (Program LUNE), at the time of observation. Another program (Program CELPS) takes the observed altitudes, azimuths, atmospheric

pressures, and temperatures for as many as six observations, along with the equatorial geocentric coordinates computed for the celestial bodies by the other programs, and computes the following:

- a. The correction for atmospheric refraction to be applied to the observed altitude, determined from the Pulkova formulation,
- b. The latitude and longitude of the intersection of every two lines of position, determined by an iterative solution of two nonlinear equations,
- c. The latitude and longitude of the center of a circle inscribed into each triangle determined by three lines of position, along with the radius of that circle in nautical miles,
- d. The perpendicular distance from each line of position to the central position of the smallest triangle in nautical miles,
- e. The latitude and longitude determined by a least squares solution of all line of position,
- f. The azimuth of the zero line of the theodolite horizontal circle referenced to true north, and
- g. The average times of all intersections and triangles determined from the original times of the observations comprising them, and the duration of the fix in hours.

Fig. 23



The final accuracy of the positions is variable. For uniform atmospheric conditions, and celestial bodies at intermediate altitudes, the positions appear to be considerably better than 0.1 nautical mile, while for some summer observations of the sun at low angles with anomalous refraction conditions, and with questionable assumptions about irradiation, the errors are on the order of 0.5 nautical mile.

For the satellite positions, the availability of each satellite on every orbit results in numerous positions, but the high fix density and slow rate of advance of the ice result in many fixes being rejected because even slightly erroneous fixes clearly lie off the well-defined track. Approximately 50% of the fixes were finally rejected. The accuracy of the acceptable fixes is generally much better than 0.1 nautical mile. Between fixes the interpolated positions are considered to be better than 0.3 nautical mile with some errors during particularly adverse conditions (high winds in storms with several days between fixes) up to 5 miles or more.

The island azimuth for the period is shown in Figure 23. This plot was obtained by computing the azimuth of the island reference line (a fictitious fiducial line on the island parallel to the 0-180° line of the theodolite horizontal circle) for each observation, using position information from the final drift track. More than 6600 observations were used. The total rotation of the island during the period was 4,672 degrees.

Table 3 presents the statistics for the drift track. The net distance is the distance made good over the month, the total distance is the overall distance between hourly positions. The meandering coefficients are normal and inverse ratios of net distance to total distance. The yearly overall distances and cumulative distances are also tabulated, as well as the average daily distance travelled for the year. The total cumulative distance for the 2587 day period was 9297 nautical miles, with an average speed of 3.59 nm/day.

II. Depth Soundings

From May 12, 1962 to June 6, 1963, 617 depth soundings were obtained using explosive sound sources and a geophone detector. After June 8, 1963, soundings were obtained once each second using a Precision Depth Recorder (PDR) and a 12 KHz Giffit sonar transceiver. These records were digitized at all slope changes, and depths computed by digital computer. More than 35,000 new soundings were determined in this manner. All were corrected using the sound velocity correction tables of Matthews (1939), and are considered to be accurate to ± 2 meters.

The soundings are shown in Figures 24 through 31 on the lowest plot. Breaks in the plot indicate a lapse of more than eight hours between soundings.

TABLE 3

DRIFT TRACK STATISTICS - FLETCHER'S ICE ISLAND (T-3)

14 MAY 1962 THROUGH 12 JUNE 1969

TIME		MONTHLY DISTANCE (NM)			MEANDERING		YEARLY DISTANCE	
MO	YEAR	NET	TOT	CUM	COEFFICIENTS		TOTAL	PER DAY
5	1962	55.02	78.51	78.51	0.70086	1.42681		
6	1962	76.75	127.58	206.09	0.60162	1.66216		
7	1962	95.50	168.42	374.51	0.56703	1.76355		
8	1962	77.23	157.35	531.87	0.49086	2.03723		
9	1962	53.45	231.66	763.53	0.23073	4.33392		
10	1962	110.23	171.29	934.83	0.64351	1.55396		
11	1962	27.54	133.75	1068.58	0.20594	4.85563		
12	1962	35.98	123.59	1192.17	0.29115	3.43464	1192.17	5.14 (232 Days)
1	1963	37.94	88.68	1280.86	0.42783	2.33733		
2	1963	36.44	81.08	1361.94	0.44945	2.22491		
3	1963	12.23	87.67	1449.62	0.13954	7.16609		
4	1963	24.77	109.49	1559.11	0.22630	4.41873		
5	1963	21.00	99.08	1658.20	0.21195	4.71787		
6	1963	10.06	83.14	1741.34	0.12109	8.25788		
7	1963	44.39	108.17	1849.52	0.41042	2.43648		
8	1963	56.15	120.74	1970.26	0.46505	2.15027		
9	1963	89.63	146.50	2116.76	0.61186	1.63433		
10	1963	87.47	144.38	2261.14	0.60588	1.65046		
11	1963	38.45	125.31	2386.46	0.30689	3.25844		
12	1963	65.78	124.99	2511.45	0.52627	1.90016	1319.28	3.61
1	1964	49.58	79.37	2590.82	0.62471	1.60073		
2	1964	26.89	56.39	2647.22	0.47686	2.09701		
3	1964	13.65	85.25	2732.48	0.16020	6.24213		
4	1964	11.12	74.76	2807.25	0.14873	6.72328		
5	1964	34.49	109.48	2916.73	0.31507	3.17382		
6	1964	10.69	129.64	3046.38	0.08250	12.12106		
7	1964	29.02	108.47	3154.86	0.26756	3.73737		
8	1964	13.58	72.54	3227.40	0.18732	5.33836		
9	1964	22.72	102.76	3330.17	0.22112	4.52227		
10	1964	34.13	110.98	3441.15	0.30755	3.25144		
11	1964	99.96	153.21	3594.36	0.65248	1.53260		
12	1964	52.35	89.96	3684.33	0.58190	1.71849	1172.88	3.20
1	1965	34.80	81.30	3765.63	0.42806	2.33609		
2	1965	44.50	70.50	3836.14	0.63118	1.58431		
3	1965	13.10	88.86	3925.00	0.14751	6.77901		
4	1965	6.27	70.07	3995.07	0.08958	11.16245		
5	1965	18.49	98.84	4093.91	0.18715	5.34312		
6	1965	45.20	85.88	4179.79	0.52635	1.89985		
7	1965	36.51	101.72	4281.52	0.35894	2.78592		
8	1965	43.46	105.19	4386.71	0.41323	2.41990		
9	1965	63.85	118.49	4505.21	0.53885	1.85577		
10	1965	37.03	155.49	4660.70	0.23815	4.19888		
11	1965	88.63	141.39	4802.09	0.62686	1.59523		
12	1965	9.98	97.55	4899.65	0.10231	9.77338	1215.32	3.33

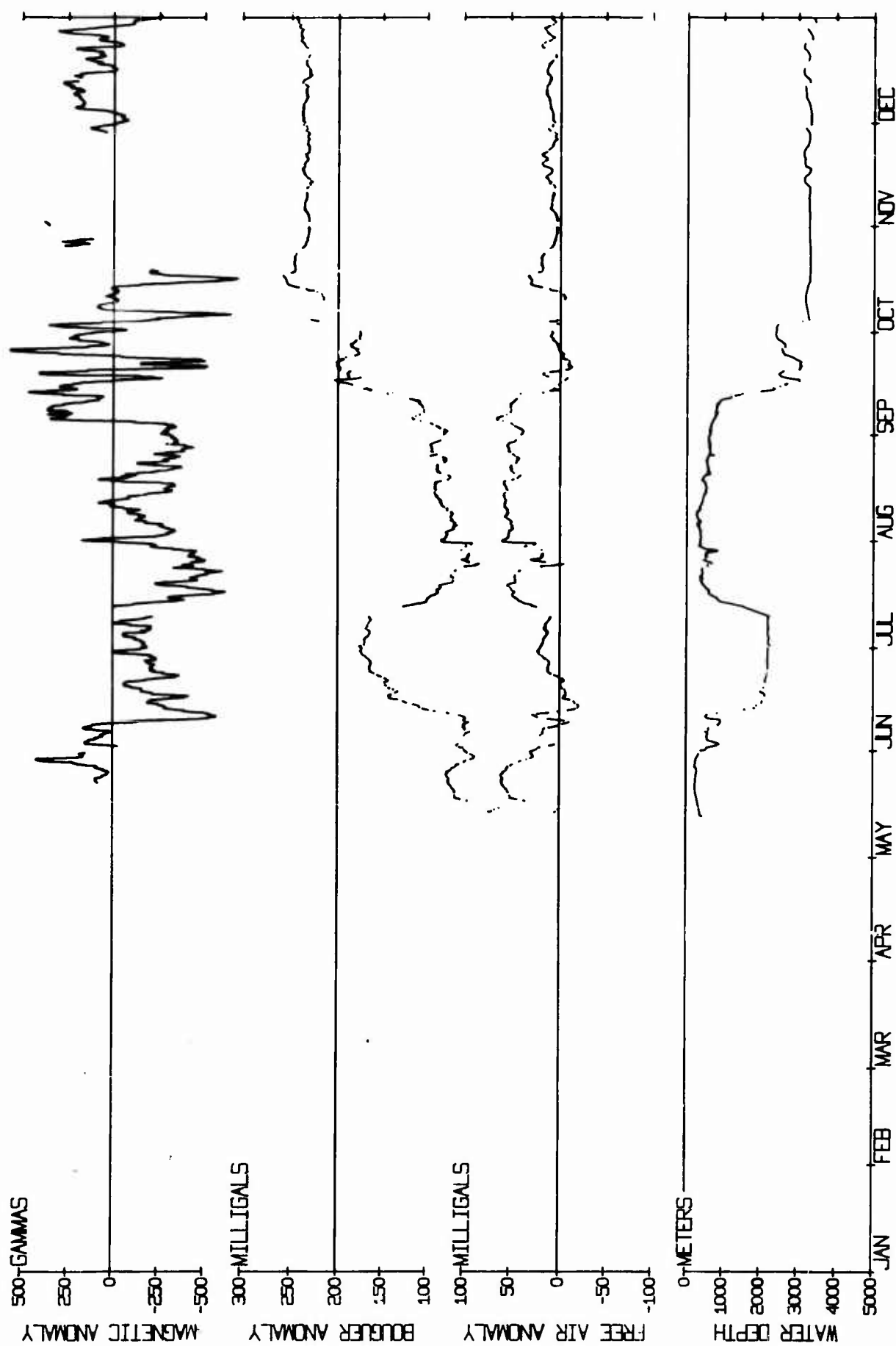
TABLE 3 (Cont'd.)

DRIFT TRACK STATISTICS - FLETCHER'S ICE ISLAND (T-3)

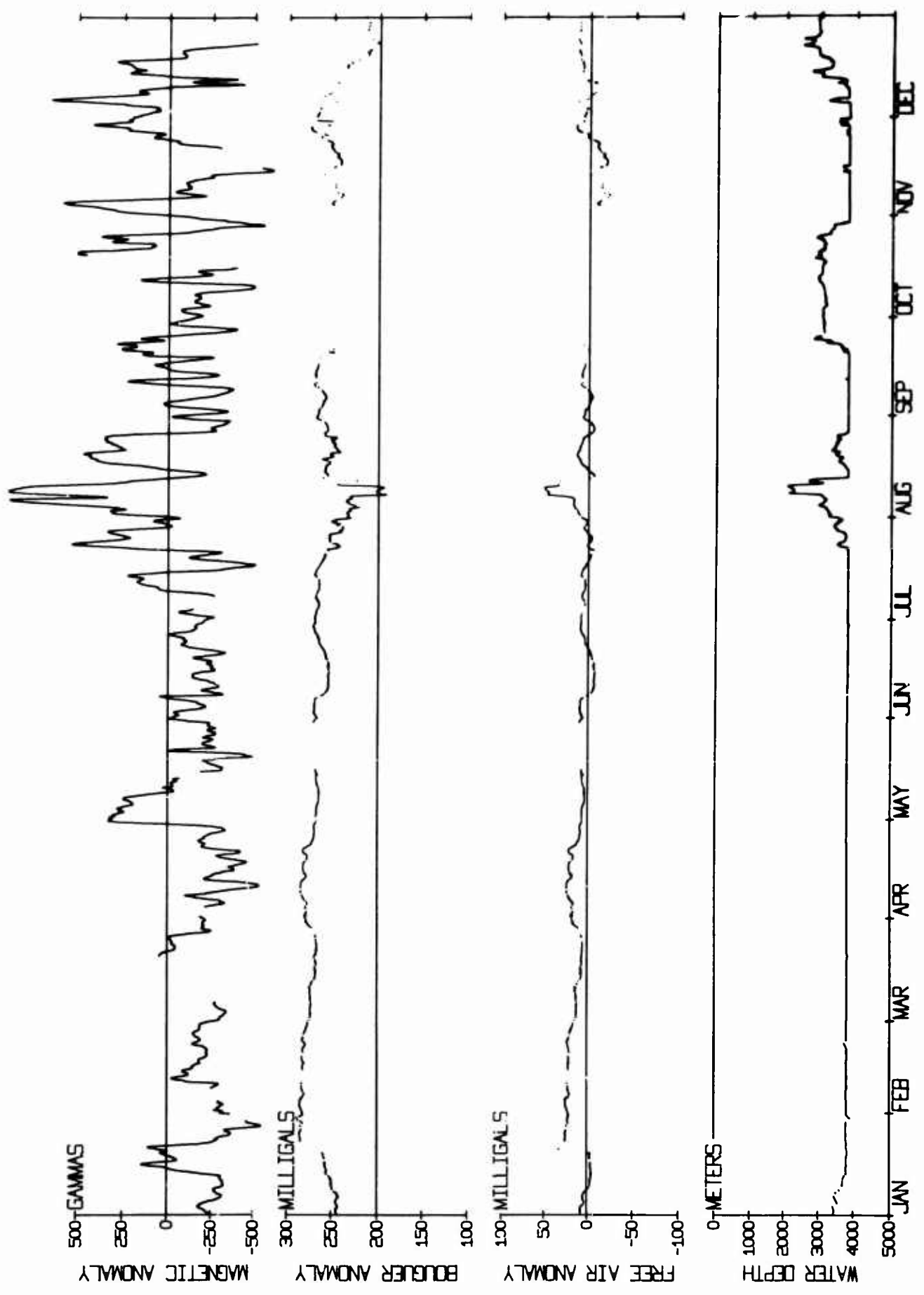
14 MAY 1962 THROUGH 12 JUNE 1969

TIME		MONTHLY DISTANCE (NM)			MEANDERING		YEARLY DISTANCE	
MO	YEAR	NET	TOTAL	CUM	COEFFICIENTS		TOTAL	PER DAY
1	1966	75.92	147.30	5046.95	0.51540	1.94020		
2	1966	59.26	119.48	5166.43	0.49600	2.01612		
3	1966	41.72	90.99	5257.42	0.45850	2.18100		
4	1966	15.12	66.16	5323.57	0.22866	4.37324		
5	1966	23.38	117.18	5440.75	0.19954	5.01145		
6	1966	51.60	125.63	5566.39	0.41078	2.43434		
7	1966	3.11	106.60	5672.99	0.02923	34.20559		
8	1966	85.64	151.81	5824.80	0.56515	1.77260		
9	1966	106.92	158.74	5983.55	0.67355	1.48466		
10	1966	97.29	132.02	6115.57	0.73692	1.35699		
11	1966	100.74	188.16	6303.73	0.53540	1.86773		
12	1966	40.15	106.20	6409.94	0.37806	2.64505	1510.29	4.14
1	1967	67.08	116.17	6526.11	0.57746	1.73169		
2	1967	12.35	78.81	6604.92	0.15679	6.37795		
3	1967	7.96	90.88	6695.81	0.08765	11.40887		
4	1967	51.69	127.17	6822.98	0.40651	2.45992		
5	1967	20.02	128.27	6951.25	0.15613	6.40453		
6	1967	21.10	118.76	7070.01	0.17768	5.62805		
7	1967	19.31	116.85	7186.86	0.16525	6.05110		
8	1967	14.51	158.78	7345.65	0.09140	10.94029		
9	1967	51.41	108.75	7454.40	0.47281	2.11499		
10	1967	65.05	140.47	7594.87	0.46311	2.15931		
11	1967	4.33	105.02	7699.90	0.04130	24.20799		
12	1967	1.31	102.27	7802.17	0.01282	77.98248	1392.23	3.81
1	1968	57.51	130.18	7932.35	0.44183	2.26327		
2	1968	17.58	65.03	7997.39	0.27043	3.69775		
3	1968	30.37	78.08	8075.47	0.38895	2.57100		
4	1968	16.79	67.32	8142.79	0.24943	4.00912		
5	1968	45.35	97.53	8240.32	0.46499	2.15057		
6	1968	26.85	80.94	8321.27	0.33177	3.01410		
7	1968	52.40	96.10	8417.37	0.54532	1.83377		
8	1968	40.71	109.09	8526.45	0.37328	2.67894		
9	1968	35.41	91.66	8618.11	0.38631	2.58858		
10	1968	50.51	106.74	8724.85	0.47321	2.11320		
11	1968	98.02	115.92	8840.77	0.84558	1.18261		
12	1968	47.10	93.00	8933.77	0.50645	1.97449	1131.60	3.09
1	1969	7.84	74.32	9008.10	0.10553	9.47569		
2	1969	20.51	71.95	9080.05	0.28510	3.50744		
3	1969	9.79	52.51	9132.57	0.18644	5.36349		
4	1969	22.05	56.47	9189.04	0.39059	2.56021		
5	1969	36.23	62.75	9251.80	0.57742	1.73183		
6	1969	5.87	45.63	9297.44	0.12873	7.76759	363.67	2.23 (163 DAYS)
TOTAL DISTANCE AND DAILY TRAVEL OVER 2587 DAYS							9297.44	3.59

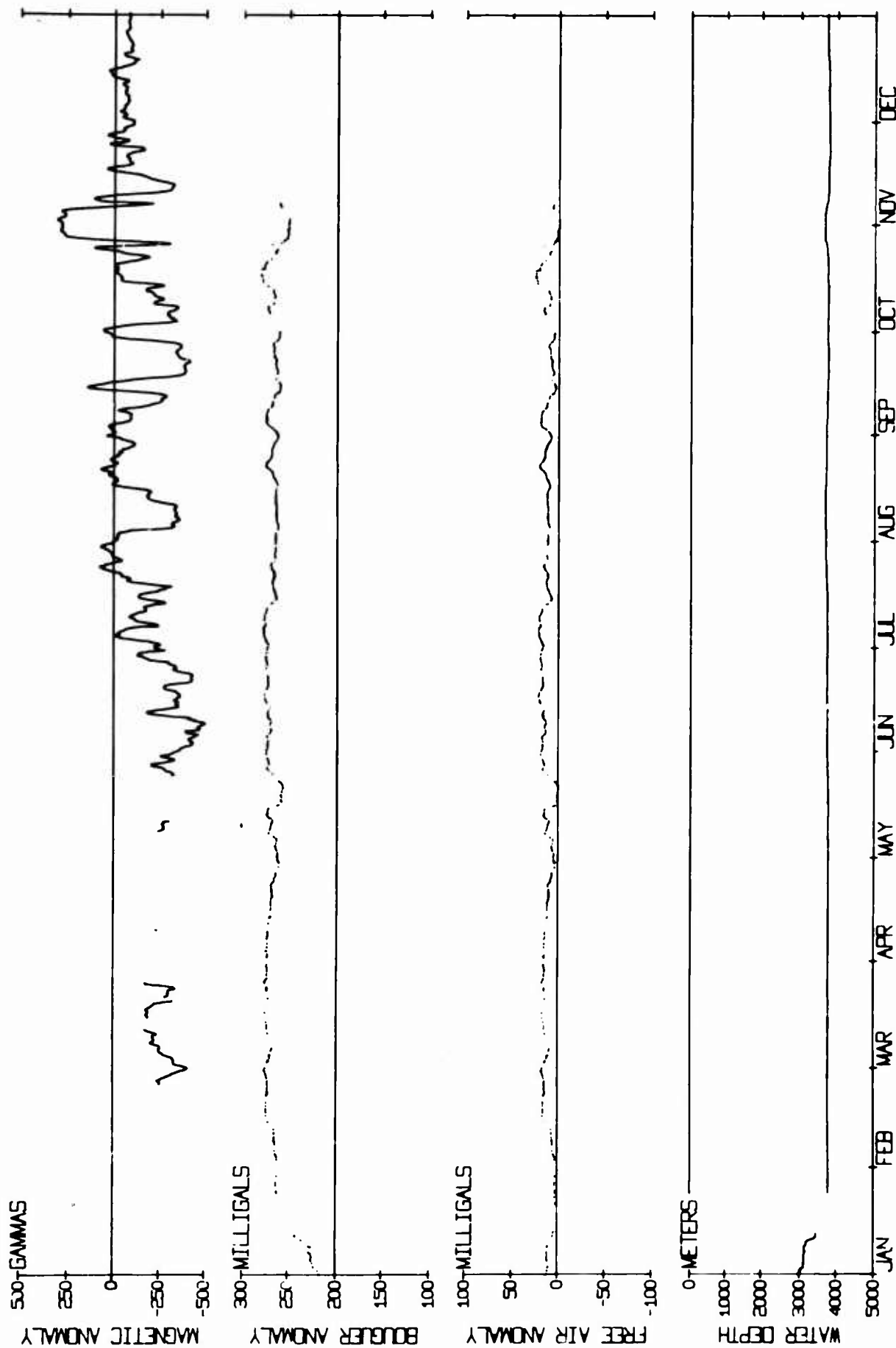
Fig. 24



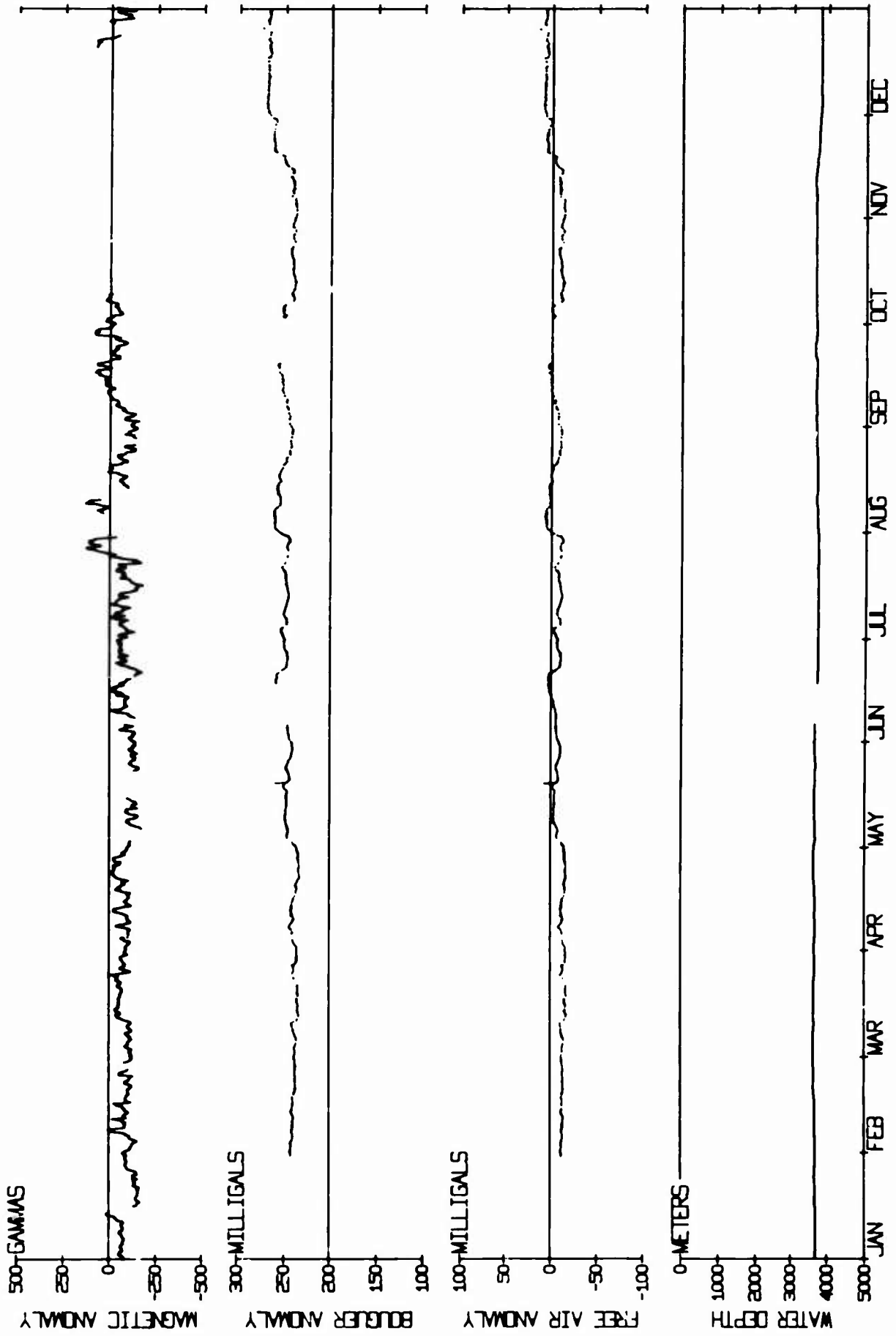
1962 GEOPHYSICAL DATA - FLETCHER'S ICE ISLAND (T-3)



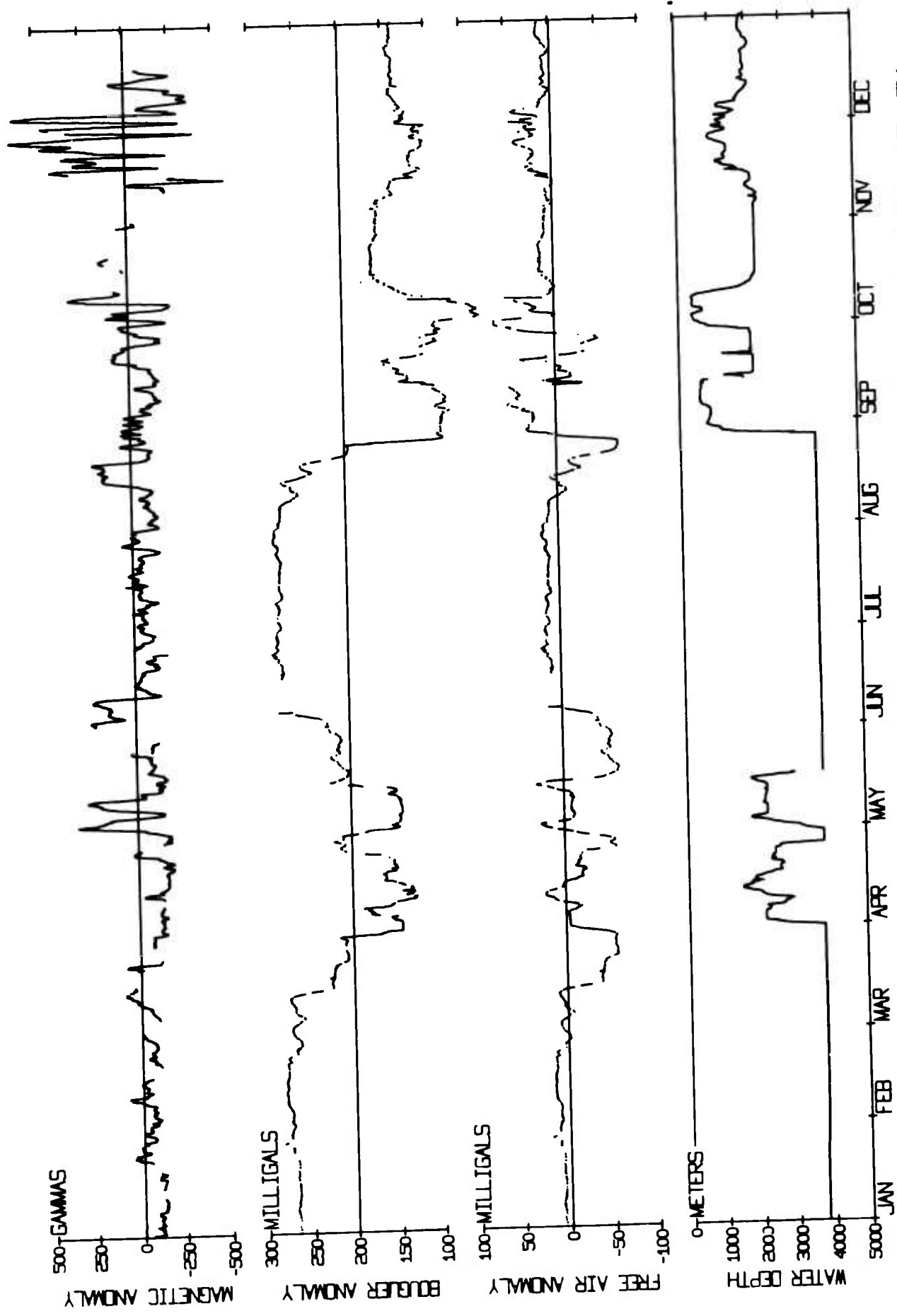
1963 GEOPHYSICAL DATA - FLETCHER'S ICE ISLAND (T-3)



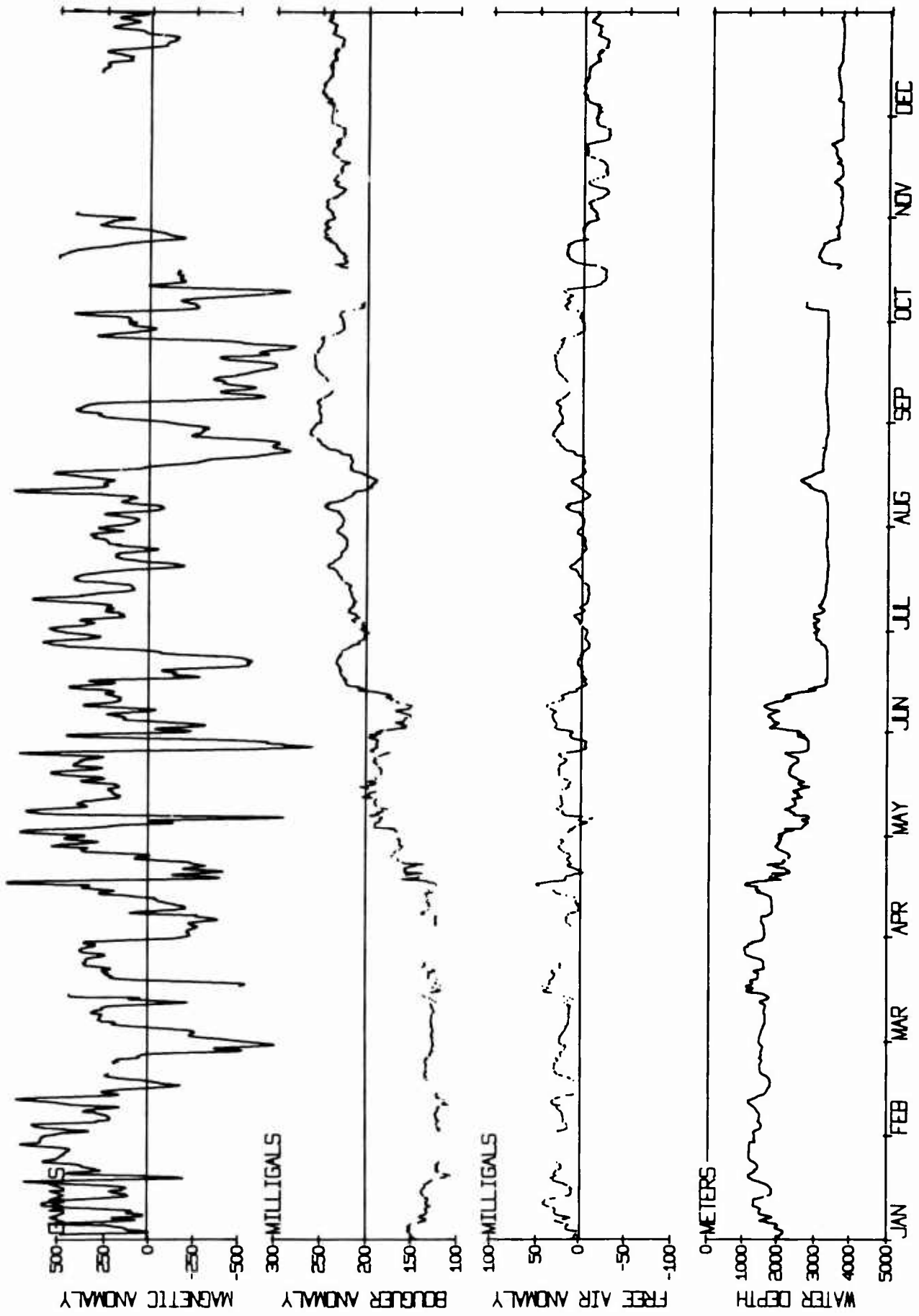
1964 GEOPHYSICAL DATA - FLETCHER'S ICE ISLAND (T-3)



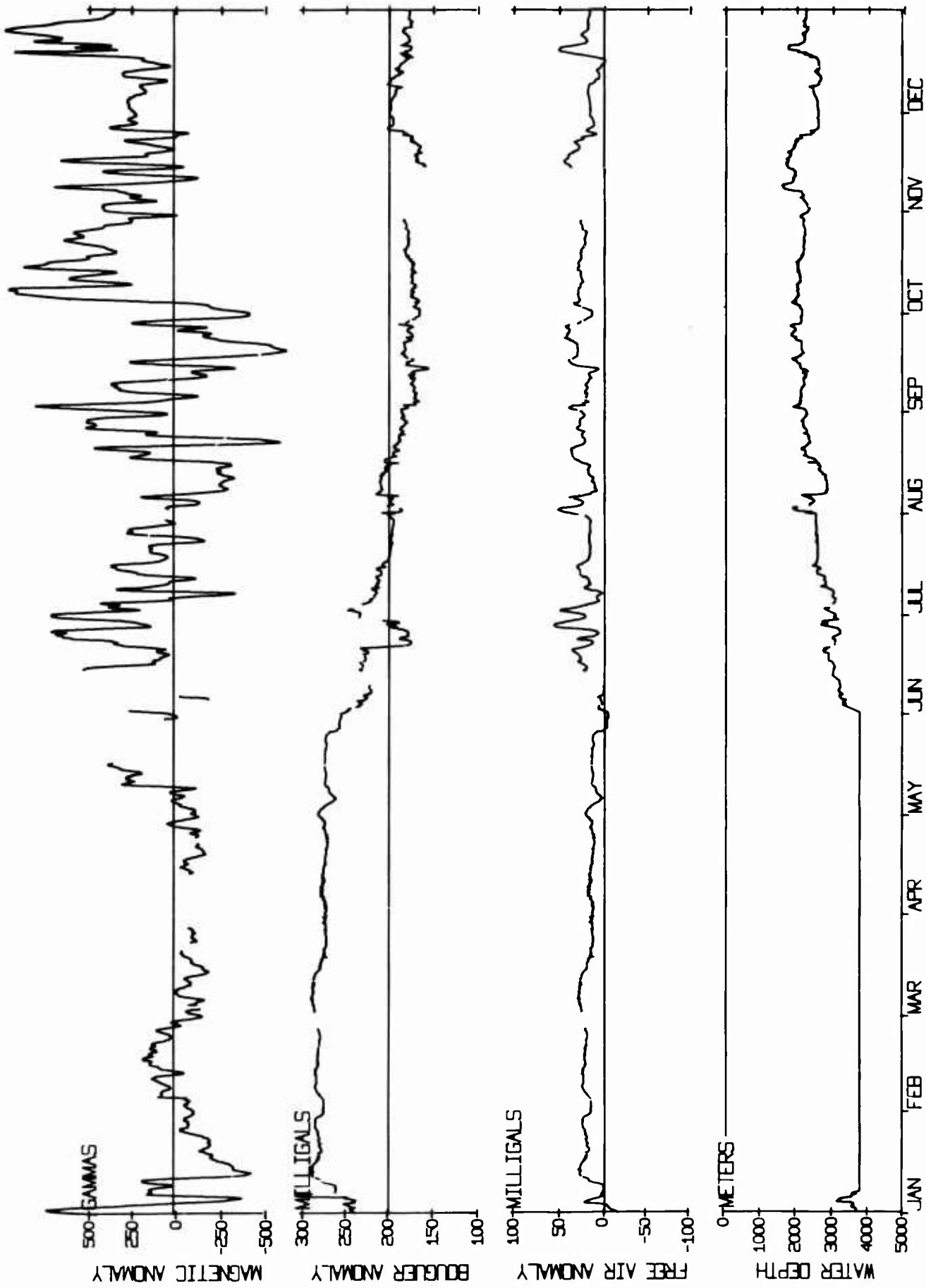
1965 GEOPHYSICAL DATA - FLETCHER'S ICE ISLAND (T-3)



1966 GEOPHYSICAL DATA - FLETCHER'S ICE ISLAND (T-3)

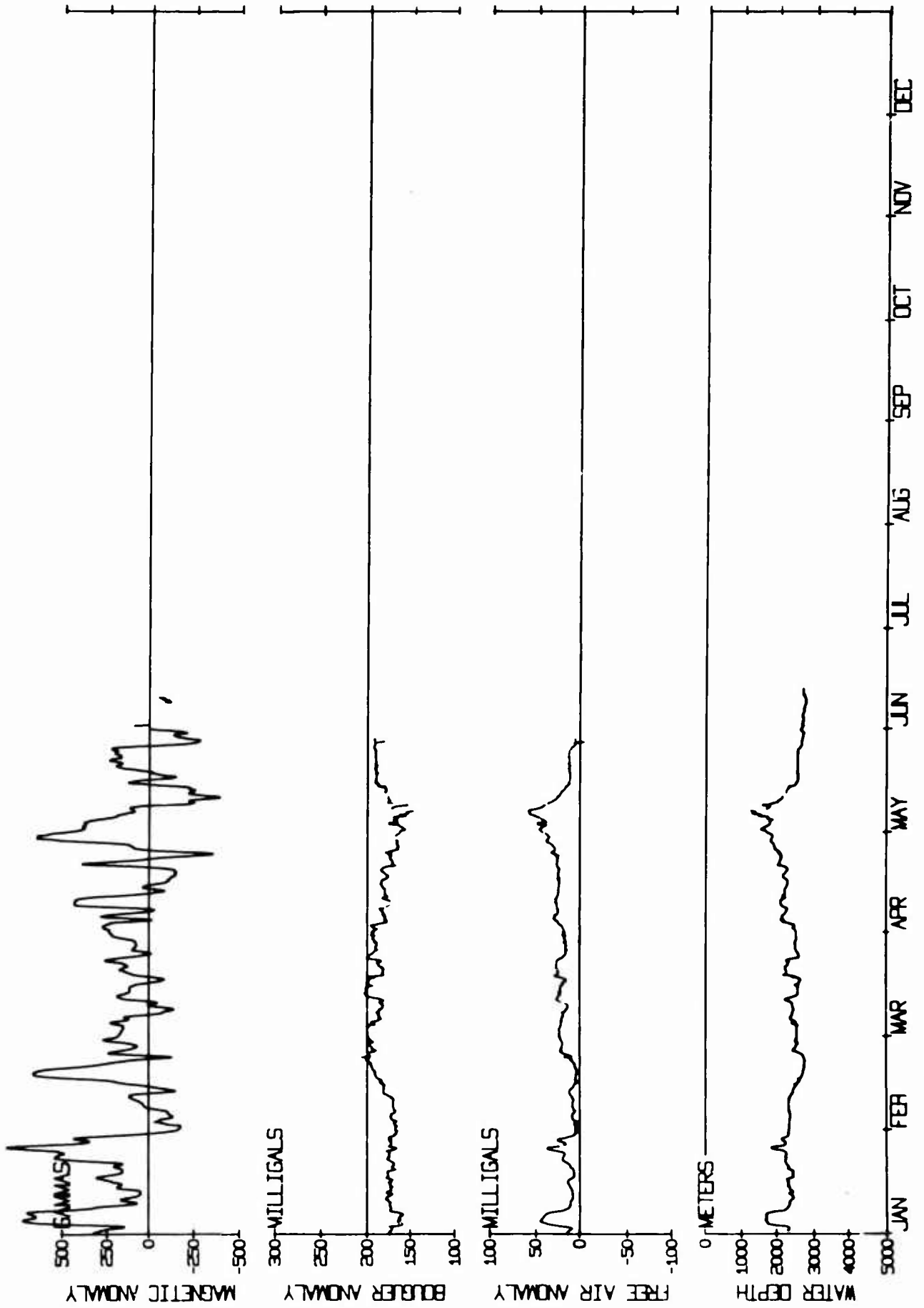


1967 GEOPHYSICAL DATA - FLETCHER'S ICE ISLAND (T-3)



1968 GEOPHYSICAL DATA - FLETCHER'S ICE ISLAND (T-3)

Fig. 31



1969 GEOPHYSICAL DATA - FLETCHER'S ICE ISLAND (T-3)

III. Magnetics

Measurements of the total magnetic field on T-3 have progressed from individual measurements with a portable Varian M-49 proton free-precession magnetometer to the present continuously recording proton instrument. Hourly observations have been digitized, converted from precession frequency to field strength, and averaged so that each new hourly value is an average for the 24-hour period centered about that hour. In this manner, because of the relatively small movement of the island, it is possible to filter out most of the large diurnal variation found in the Arctic. Magnetic anomalies were then computed by removing the regional magnetic field, computed from a recent Canadian formulation described by Haines (1967).

The magnetic anomalies are shown in Figures 24 through 31 along the uppermost plots. Breaks in the data indicate periods of more than 12 hours between observations. Of note is the striking difference between the large amplitude anomalies associated with the Mendeleev Ridge and Alpha Rise (1963 and 1967-69 data) and the low amplitude anomalies in the southern Canada Plain (1965-66 data). Nearly 50,000 observations are included in these plots.

IV. Gravity

Over 10,200 gravity observations were made during the period with a Lacoste and Romberg Model G geodetic gravity meter (number 27). The gravity meter was taken to the University of Wisconsin

pendulum station in Barrow 22 times for calibration ties. Prior to mid-October 1964, the meter showed a positive drift of less than 1.5 milligals per year, but after some large thermal shocks and a positive 30 milligal tare in late 1964, the drift became negative at slightly over 2 milligals per year.

The gravity observations were reduced by computer. One program determined the base value for the gravity meter during gravity ties. Earth-tide corrections were included, calculated from the astronomical formulae used in the navigation programs. A second program then corrects the gravity observations for instrumental drift, converts dial readings to milligals, corrects for height above sea level (free air correction) and east-west movement of the island (the Eötvös connection), and computes corrected gravitational field, free air and Bouguer anomalies. The free air and Bouguer anomalies are shown in Figures 24 through 31. The Bouguer anomalies are based on a density for the water column of 2.67 gm/cm^3 . Gaps in the record indicate periods of more than eight hours between observations, or in the case of the Bouguer anomalies, a lack of depth information.

The reading sensitivity of the gravity meter is approximately 0.01 milligal, and the instrumental drifts are sufficiently small and linear so that accuracies of 0.03 milligal should be possible.

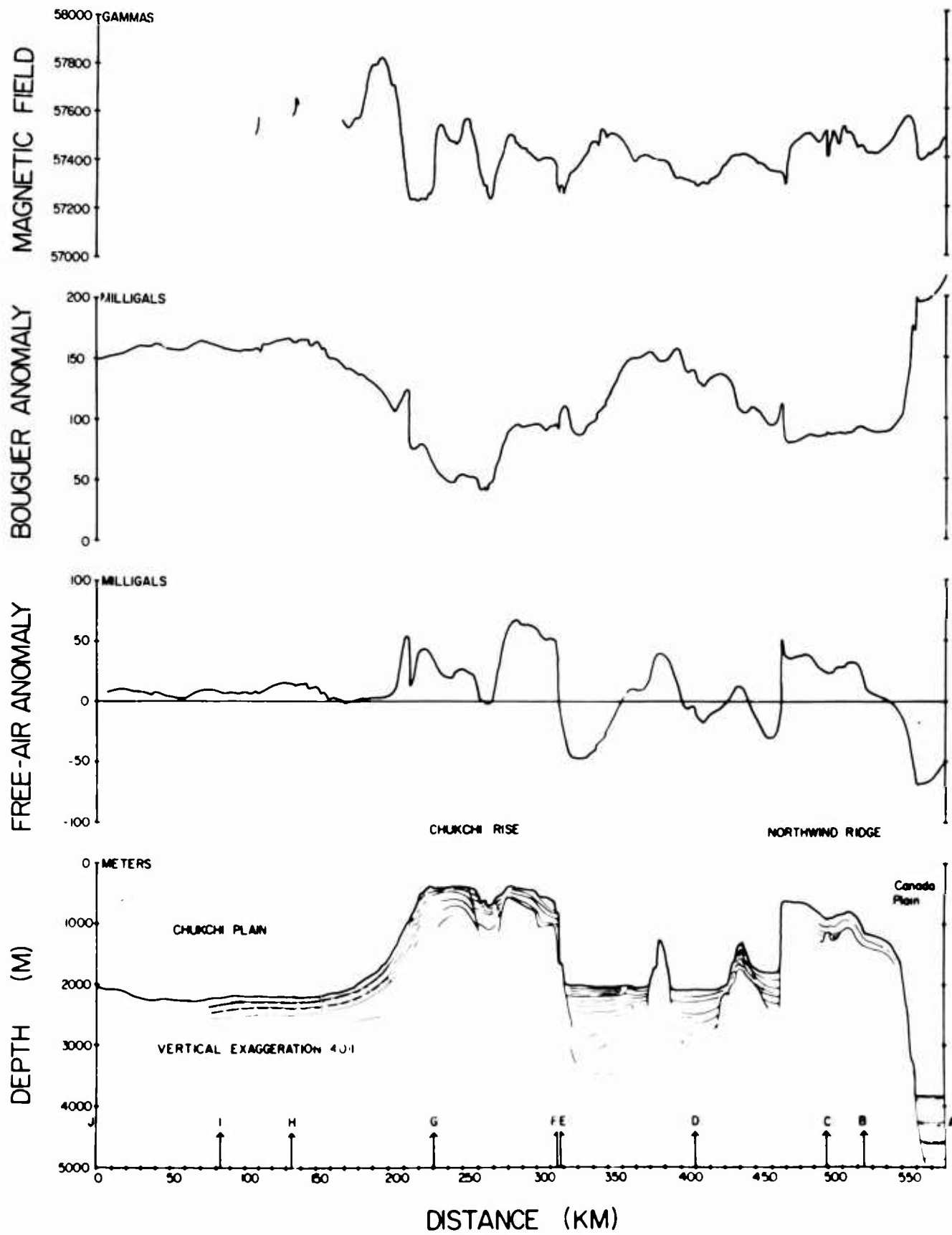
However, motions of the ice island tend to make meter readings a process of centering the reading needle oscillations, so that accuracies are probably on the order of 0.3 milligals, and possibly as bad as ± 5 milligals during storms. Eötvös corrections as large as ± 1 milligal were made, and the overall uncertainty in meter height probably amounts to 0.2 milligal or less, so that with the navigational errors, the overall accuracy is on the order of 1 milligal.

V. Sub-Bottom Profiling

A seismic profiler, using two omnidirectional hydrophones and a capacitor-discharge sound source with spark-type transducer was installed during the summer of 1966. The energy output was 9000 joules, with peak acoustic output below 100 Hz, and the repetition rate was approximately once every 300 seconds. With the exception of a five-week gap in Feb-Mar 1967, three weeks in Sept-Oct 1967, and 216 days lost between Jan and Aug 1968, operation has been continuous, with 757 days (out of 1061 days) of track being profiled. Acoustic penetration of up to 2500 meters has been achieved, and records clearly show the sedimentary structure as well as the greater-than-usual accumulation of sediments in this part of the ocean.

Figure 32, a geophysical profile across the southern half of the Northwind Ridge and the Chukchi Rise in 1966, shows the detail added to such a profile by this type of data.

Fig. 32



VI. Marine Geology/Bottom Photography

Since 1963, a Thorndike bottom camera has been used to secure photographs of the sea-floor. A nephelometer or light-scattering meter is often included to measure the turbidity of the water as a function of depth - an index of its sediment and biological content. A total of 128 lowerings have been made to date, resulting in approximately 80 usable nephelometer records, and 2067 photographs.

In the spring of 1967 a tripod-mounted camera for making close-up photos and bottom current measurements was added to the program. Three small core barrels were sometimes added at the corners of the tripod base to obtain bottom specimens. Eighty lowerings have been made with this device, 17 of them with the core barrels attached, resulting in approximately 1000 more photographs. At several stations a minnow trap fastened to the base was used to capture amphipods seen in the photos.

References Cited

Matthews, D.J., (1939), Tables of the Velocity of Sound in Pure Water and Sea Water for Use in Echo-Sounding and Sound-Ranging. Hydrographic Dept., Admiralty, London. H.D. Publ 282.

Haines, C.V., (1967), A Taylor Expansion of the Geomagnetic Field in the Canadian Arctic, Publ. of the Dominion Observatory, Vol XXXV, No. 2, Ottawa, Canada.

ABSTRACTS OF SELECTED PAPERS AND REPORTS

ISSUED UNDER NONR 266 (82)

Hall, J.K., and K. Hunkins, "A Geophysical Profile across the Southern Half of the Chukchi Rise: Arctic Ocean." AGU Spring Meeting, 1968.

ABSTRACT

Between August and November 1966, measurements of ocean depth, magnetics, gravity and sediment thickness were made across the southern half of the Chukchi Rise from drifting ice island T-3. These new observations supplement and clarify the geophysical results of earlier explorations in this general area. Precision depth recordings show the Chukchi Plain to be a true abyssal plain, and indicate the depression between the Rise and the Northwind Ridge to consist of two narrow abyssal plains differing in depth by 50 meters, and separated by a ridge 800 meters high. Seismic profiles show faulted and deformed sediments on the Chukchi Rise, and up to 800 meters of flat-lying sediments beneath the abyssal plains. The prominent magnetic anomaly on the western margin of the Chukchi Rise, which has been extensively surveyed to the north, was found to continue southward, although reduced in amplitude.

Heirtzler, J.R., "Simultaneous geomagnetic measurements on an ice island surface and 1000 feet below". Tech. Report No. 2, May 1963.

ABSTRACT

For a few weeks in the fall of 1962 the total geomagnetic field intensity was measured simultaneously on an ice island surface and approximately 1000 feet below. The magnetic gradient as indicated by the difference between the two readings varied as the station passed over geologic bodies. A statistical analysis of the time variations during two time intervals revealed an attenuation and phase shift of the lower head reading with respect to the surface head reading. The analysis was made between 70 and 400 seconds period. There are indications of an anomalous attenuation at the lower period end of this band although the experiment was not such that accurate determinations could be made.

Hunkins, K., "Waves on the Arctic Ocean". Jour. of Geophys. Res., v. 67, no. 6, June 1962.

ABSTRACT

A continuous vertical oscillation of the ice of the Arctic Ocean has been observed at four U.S. drifting research stations. In the period range of 15 to 60 sec, the oscillations were detected with seismometers and gravity meters, and the displacement amplitudes were about $\frac{1}{2}$ mm at 30 sec. Amplitudes increase roughly as the square of the period. These oscillations are, in part at least, generated by wind action. In one case, oscillations in this period range have been identified as propagating waves. Theoretical dispersion curves for propagating flexural-gravity waves are presented. Oscillations in the 10- to 100-min period range were detected with a tide recorder operating at a grounded ice station, T-3, on the continental shelf, 130 km northwest of Point Barrow, Alaska. Displacement amplitudes were about 1 cm at a period of 30 min and were roughly proportional to period. The Arctic Ocean wave spectrum contrasts with that of other oceans. The spectral peak due to sea and swell is absent, and the present data indicate a monotonic increase in displacement amplitude as the periods range from about 0.1 to 60 sec in deep water or from about 0.1 sec to 100 min on the continental shelf.

Shaver, R., and K. Hunkins , "Arctic Ocean geophysical studies: Chukchi Cap and Chukchi Abyssal Plain". Deep-Sea Research, vol. 11, pp. 905-916, 1964.

ABSTRACT

A bathymetric chart of the Chukchi Cap region was compiled with soundings obtained from Fletcher's Ice Island (T-3), as well as from other ice stations and from U.S. Navy icebreakers. New details of the Chukchi Cap are shown, including two submarine troughs on the southwest side. West of the Chukchi Cap, a small abyssal plain was found with a depth of 2230 m. This abyssal plain is connected through an abyssal gap with the deeper Canada Abyssal Plain.

The prominent magnetic anomaly discovered during the drift of Station Charlie was crossed more recently by T-3 and by aeromagnetic flights. The continuity of the anomaly along the western and northern sides of the Chukchi Cap was further established by the new measurements. An interpretation was made of the anomaly as an expression of induced magnetization in basement rocks. The interpretation shows a basement ridge beneath the anomaly maximum at the edge of the Chukchi Cap. The Cap itself is interpreted as being underlaid by a 12 km thickness of sediments. Both magnetic and gravity data were used for an interpretation of total crustal thickness along the same section. Crustal thickness ranges from 18 $\frac{1}{2}$ km beneath the Chukchi Cap to 32 km beneath the large basement ridge.

Hunkins, K., "The seasonal variation in the sound-scattering layer observed at Fletcher's Ice Island (T-3) with a 12-kc/s echo sounder". Deep-Sea Research, vol. 12, pp. 879-881, 1965.

ABSTRACT

For nearly two years, from June 1963 to the present, an echo sounder has been operated continuously at Fletcher's Ice Island (T-3), a drifting research station in the central Arctic Ocean. Diffuse reverberations are frequently seen on the echograms during the summer months. These reverberations are similar in general appearance to the deep scattering layers of other oceans.

In non-polar oceans, the deep scattering layer is usually found at depths between 200 and 600 m during the day. At night it rises almost to the surface and weakens or disappears. Two important features distinguish the Arctic Ocean scattering layers from these non-polar scattering layers: (1) the Arctic Ocean scattering layers are relatively shallow, 50-200 m, and (2) the Arctic scattering layers have a pronounced annual, rather than diurnal, cycle. These effects are probably related to light conditions peculiar to polar oceans. First, the light is relatively weak beneath the permanent ice cover. Second, the "day" becomes effectively one year long at these high latitudes so that the Arctic scattering layers are present at moderate depths during the summer light period and then disappear during the winter dark

In addition to the scattering layers, discrete echoes from shallow depths are frequently recorded. These discrete echoes occur throughout the year but are particularly frequent during the winter. These echoes take a hyperbolic shape indicating relative movement between the ice station and the reflector. Presumably they are caused by nekton such as fish or seals.

Hunkins, K., "Sound scattering layers in the Arctic Ocean observed from Fletcher's Ice Island (T-3)", to be published in the Proceedings of the 6th Annual Symposium on Military Oceanography.

ABSTRACT

Continuous observations of sound scattering layers have been made in the Arctic Ocean from Fletcher's Ice Island (T-3) since 1963 with a 12 kHz sounder. A characteristic diffuse scattering layer between the depths of 25 and 200 m was observed in the summers of 1963, 1964, 1965 and 1968 but not during the summers of 1966 and 1967. Since the ice island drifts continually, the measurements may indicate a spatial variation in this scattering layer which is superimposed on a seasonal cycle. The layer also varies diurnally, particularly at the time of the equinoxes when the maximum light contrast between day and night occurs.

Observations with a 100 kHz sounder in 1967 and 1968 showed that many individual scatterers are present in the upper layers even when no diffuse layer is observed at 12kHz. The 100 kHz sounder was also able to resolve individual scatterers in the same layer which appeared cloud-like on the 12 kHz.

In addition, the 100 kHz records show a persistent layer at a depth of about 50 m. This thin scattering layer coincides with the base of the homogeneous mixed layer. Tests are being made to

determine whether this layer is caused by specular reflection from the density discontinuity or whether it is due to sound scattering from organisms or debris at that level.

Hunkins, K., E. Thorndike and G. Mathieu, "Nepheloid layers and bottom currents in the Arctic Ocean" (in press).

ABSTRACT

Between 1965 and 1969, 51 profiles of light scattering were made in the central Arctic Ocean from Fletcher's Ice Island (T-3). The profiles, taken with an in situ photographic nephelometer extend from just below the surface to the bottom.

Two distinctly different types of profiles were observed. At all stations the strongest scattering occurs near the surface, decreasing with depth in the upper layers. Over the Canada Abyssal Plain, light scattering is almost constant below 2000 m, decreasing slightly with depth all the way to the bottom so that the bottom water is the clearest. But over the ridges and rises surrounding the Canada Basin scattering increases with depth below an intermediate scattering minimum. The zone of deep light scattering on the ridges and rises is called the bottom nepheloid layer.

The bottom nepheloid layer is evidently caused by fine material which is maintained in suspension by the turbulent flow. Four spot measurements of bottom currents on the Mendeleev Ridge gave speeds of 4 to 6 cm/sec. One spot measurement over the Canada Abyssal Plain gave a speed of less than 1 cm/sec. This indication of

swifter current speeds over the ridges is supported by bottom photographs in which animal tracks are much less evident on the ridges than on the Canada Abyssal Plain in spite of a greater abundance of life on the ridges. This is attributed to the higher current speeds which obliterate the tracks.

The observations suggest a counterclockwise deep circulation in the Canada Basin with the currents confined primarily to the sloping margins of the basin. This pattern of deep circulation is in agreement with ideas and experiments on deep circulation with a concentrated source and distributed surface sink. Deep water enters the basin over a sill and leaves by upward diffusion through the halocline into the surface water which then flows out of the basin.

Kutschale, H., "Arctic Ocean Geophysical Studies: The Southern Half of the Siberia Basin", *Geophysics*, vol. XXXI, no. 4, 1966.

ABSTRACT

In 1962, ice island Arlis II drifted over a portion of the southern half of the Siberia Basin. Depth recordings made between 81°N , 170°E and $82^{\circ}30'\text{N}$, 160°E show that the ocean floor in this area is an abyssal plain at about 2,825 m depth dissected by several interplain channels. This abyssal plain, here called the Wrangel Abyssal Plain, is bounded on the north by Arlis Gap, which joins it with the Siberia Abyssal Plain at about 3,946 m depth. The Siberia Abyssal Plain occupies the northern half of the Siberia Basin. Seismic reflection profiles show that a prominent subbottom basement ridge exists in the vicinity of Arlis Gap. This ridge strikes in an approximately northwest direction and appears to connect with Alpha Ridge, which bounds the Siberia Basin on the east and north, and with Lomonosov Ridge, which bounds the Siberia Basin on the west. The seismic reflection profiles also show that at least 3.5 km of subhorizontal, stratified sediments underlie Wrangel Abyssal Plain south of the ridge. Each layer within these sediments appears to correspond to a fossil surface of Wrangel thick Abyssal Plain. This/sequence of stratified sediments shows the influence of the Asian continent, which bounds the Siberia Basin

on the south, on sedimentation within the Siberia Basin. Presumably the buried basement ridge forms a dam which has permitted the accumulation of a thick sequence of sediments under the higher-level Wrangel Abyssal Plain. Turbidity currents moving through Arlis Gap presumably carried the overflow of sediments from Wrangel Abyssal Plain into the lower-level Siberia Abyssal Plain. The structure of the sediments suggests that the Siberia Basin has been free from deformation during the deposition of the sediments, except for possible broad crustal down warping. A crustal model based on the water depth measurements, seismic reflection profiles, gravity measurements, and magnetic measurements yields a crustal thickness of 15 km south of the buried ridge and 22 km under the ridge measured from sea level.

Hunkins, K., "Ekman drift currents in the Arctic Ocean".
Deep-Sea Research, vol. 13, pp. 607-620, 1966.

ABSTRACT

Current observations from a drifting ice floe in the central Arctic Ocean give clear evidence of a clockwise spiral structure in the upper layers. The data for steady conditions show a boundary layer just beneath the ice and an Ekman spiral layer below it. The depth of frictional influence is 18 m for winds of 4 m/sec. This is apparently the first detailed confirmation of the Ekman spiral in deep waters.

Hunkins, K., "Inertial Oscillations of Fletcher's Ice Island (T-3)", Jour. of Geophys. Res., vol. 72, no. 4, 1967.

ABSTRACT

Observations with improved Roberts current meters, tethered drogues, and fathogram highlights are used to show that Fletcher's Ice Island (T-3), in the Arctic Ocean, often moves in clockwise circles with a diameter of about 1 km and a period of about 12 hours. The motions are inertial oscillations which represent the transient response of a floating ice mass to changing wind stress. Since the winds are often fluctuating, T-3 responds often with inertial motion. The following arguments indicate that these motions are inertial oscillations: (1) the period of the motions is closer to the inertial period, at this latitude, of 12.05 hr than it is to the lunar semidurnal tidal period of 12.42 hr; (2) the amplitude of the periodic motion and the local wind speed are closely correlated; (3) the phase of the motion changes irregularly with time; and (4) the motion is restricted to the ice and to the uppermost layers of water.

Hunkins, K., and H. Kutschale, "Quaternary Sedimentation in the Arctic Ocean", in Progress in Oceanography, vol. 4, ed. M. Sears, 1967.

ABSTRACT

A distinct boundary between sediment types usually occurs at a depth of about 10 cm in bottom cores raised from the Alpha Rise in the Arctic Ocean. The sediment between the tops of the cores and the 10 cm boundary is a dark brown, foraminiferal lutite mixed with ice-rafted sand and pebbles. The sediment between the 10 cm boundary and a depth of about 40 cm is a light brown sand with ice-rafted material but few Foraminifera. The 10 cm boundary apparently represents the most recent change in pelagic deposition in this region and must be connected with climatic changes. Foraminifera from a zone between 7 and 10 cm have been dated by the C^{14} method as $25,000 \pm 3000$ and as 30,000 years BP in two different samples. The 10 cm boundary itself has been dated as 70,000 years BP by a uranium series method. If these dates are accepted, a low sedimentation rate of $1\frac{1}{2}$ to 3 mm/1000 years is indicated for the Alpha Rise and for the Arctic Ocean as a whole if pelagic sedimentation has been uniform over the entire ocean. Cores from the Canada Abyssal Plain differ in character from the Alpha Rise cores consisting primarily of olive-gray lutite without Foraminifera or ice-rafted material. This sediment

was probably deposited by turbidity currents. A 3 mm layer of dark brown, foraminiferal lutite occurs at the top of the Canada Abyssal Plain cores. This layer is similar to the upper layer in Alpha Rise cores and apparently represents continued pelagic deposition since the last turbidity current. Foraminifera from this upper 3 mm layer have been dated as 700 ± 100 years BP by the C^{14} method. The conclusion is that pelagic sedimentation has continued unchanged in the Arctic Ocean from about 70,000 years ago to the present. This implies that the present ice cover has existed for that length of time.

Kutschale, H., "Seismic Studies on Ice Island Arlis II"
Reprinted from ARCTIC DRIFTING STATIONS: A report
on Activities Supported by the Office of Naval
Research. J.E. Sater, Coordinator. 1968 by The
Arctic Institute of North America.

ABSTRACT

From May 1961 to May 1965 a scientific research station was maintained aboard a drifting ice island in the Arctic Ocean and the Greenland Sea by the Arctic Research Laboratory, Barrow, Alaska, under contract with the Office of Naval Research. This ice island was named ARLIS II, which is short for Arctic Research Laboratory Ice Station Two. Thomas (1965) gives an interesting account of the history of the island and life of personnel aboard the island. During the 4-year period of its occupancy, ARLIS II moved across the central Arctic Ocean and then through the Greenland Sea, from a point about 180 km north of Pt. Barrow, Alaska, to a point about 100 km west of Iceland, where the station was evacuated preceding its disintegration and subsequent melting. The research programs carried out aboard ARLIS II included oceanography, studies of the physical properties of sea ice and sea-ice movement, micrometeorology, geological studies of the ice island, marine geophysics, and seismic and underwater-acoustic studies. Members of the Lamont Geological Observatory of Columbia University carried out programs in marine geophysics and seismic and underwater-acoustic studies.

The present paper presents the results of seismic experiments made aboard ARLIS II to study elastic wave propagation and to determine the elastic constants and thicknesses of this ice body. The experiments were made during the summer of 1961 as the island moved under the influence of winds and currents over the Chukchi Shelf and the bordering continental margin northwest of Pt. Barrow, Alaska.

Prentiss, D., E. Davis and H. Kutschale, "Natural and man-made ice vibrations in the central Arctic Ocean in the frequency range from 0.1 to 100 cps", Tech Rept. No. 4, Jan. 1965.

ABSTRACT

During April and May, 1962, ice vibrations in the frequency range from 0.1 to 100 cps were measured aboard drifting ice island ARLIS II in the central Arctic Ocean. A vertical-component seismometer, which was anchored to the surface of the island, was employed as a detector. Typical displacement spectra show the following characteristics:

- (1) a nearly constant decrease in amplitude with increasing frequency from 2.4×10^4 μ at 0.1 cps to 1.0 μ at 6 cps
- (2) an amplitude minimum of 0.1 μ between 6 and 10 cps
- (3) an amplitude peak of 2 μ between 30 and 70 cps.

The data show some correlation between local wind speed and the amplitudes of ice vibrations. Under the quietest conditions, which correspond to minimum local wind, the ice surface in the frequency band 1 to 10 cps is quieter than a quiet land site. Under the most unfavorable conditions ambient vibrations in the frequency range from 30 to 80 cps approach those measured at noisy land sites. Local ice tremors, caused by ice fracture, enhance vibrations in the frequency range between 0.7 to 10 cps. These transient signals do not interfere significantly with SOFAR signal

detection because of their short duration and characteristic dispersion. In a general way, the amplitude spectra of both local and SOFAR shots are in most cases strikingly similar to the ambient vibration spectra. In the 10-20 cps band the reverberation spectra rise smoothly from 6 to 10 db above the ambient level and are apparently independent of shot size, depth, and propagation path.

BIBLIOGRAPHY OF SCIENTIFIC PAPERS:

Supported Under Contract Nonr 266(82)

- Beal, M.A., F. Edvalson, K. Hunkins, A. Molloy, and N. Ostenso,
1966. The floor of the Arctic Ocean: geographic names.
Arctic, 19(3), pp. 214-219.
- Demenitskaya, R.M., and K. Hunkins, 1969. Shape and structure
of the Arctic Basin. A chapter for "The Sea", vol. 4,
ed. by A. Maxwell (in preparation).
- Heirtzler, J.R., 1967. Measurements of the vertical geomagnetic
field gradient beneath the surface of the Arctic Ocean.
Geophys. Prospect., 15 (2), pp. 194-203.
- Hunkins, K., 1963. Arctic submarine acoustics in Proceedings of
the Arctic Basin Symposium, Oct. 1962. Arctic Institute of
North America, pp. 197-205.
- Hunkins, K., 1963. Submarine structure of the Arctic Ocean from
earthquake surface waves, in Proceedings of the Arctic Basin
Symposium, Oct. 1962. Arctic Institute of North America,
pp. 3-8.
- Hunkins, K., 1965. The seasonal variation in the sound-scattering
layer observed at Fletcher's Ice Island (T-3) with a 12 kc/5
echo sounder. Deep-Sea Research, vol. 12, pp. 879-881.
- Hunkins, K., 1966. The Arctic continental shelf north of Alaska,
in Continental Margins and Island Arcs, ed. by W.H. Poole,
Geol Survey of Canada, Paper 66-15, pp. 197-205.

- Hunkins, K., 1966. Ekman drift currents in the Arctic Ocean, Deep-Sea Research, vol. 13, pp. 607-620.
- Hunkins, K., 1966. The deep scattering layer in the Arctic Ocean, U.S. Navy Jour. of Underwater Acoustics, vol. 16(2), pp. 323-330.
- Hunkins, K., 1967. The Central Polar Basin in Naval Arctic Manual ATP-17A, Part I, Environment. Prepared by Arctic Institute of North America for Department of National Defense, Montreal Chap. 12.
- Hunkins, K., 1967. Inertial oscillations of Fletcher's Ice Island (T-3), J. Geophys. Res., vol. 72(4), pp. 1165-1174.
- Hunkins, K., 1968. Geomorphic provinces of the Arctic Ocean, in Arctic Drifting Stations, AINA, Wash. D.C., pp. 365-376.
- Hunkins, K., 1969. "Arctic Geophysics" to be published in the Proceedings of the Naval Arctic Research Laboratory, Dedication Symposium, April 1969, Fairbanks, Alaska.
- Hunkins, K., 1969. "Sound-scattering layers in the Arctic Ocean observed from Fletcher's Ice Island (T-3)" to be published in the Proceedings of the 6th Annual Symposium on Military Oceanography.
- Hunkins, K., and H. Kutschale, 1963. Shallow-water propagation in the Arctic. J. Acous. Soc. Am., vol. 35(4), pp. 542-551.
- Hunkins, K., and H. Kutschale, 1967. Quaternary sedimentation in the Arctic Ocean, in Progress in Oceanography, vol. 4, editor Mary Sears, Pergamon Press, 89-94.

- Hunkins, K., E. Thorndike and G. Mathieu, 1969. Nepheloid layers and bottom currents in the Arctic Ocean (in preparation).
- Jacobs, M.B., and M. Ewing, 1968. Concentration of suspended particulate matter in the major oceans. *Science* (in press).
- Kutschale, H. 1966. Arctic Ocean geophysical studies: the southern half of the Siberia Basin, *Geophysics*, XXXI (4), pp. 683-710.
- Kutschale, H., 1968. Seismic studies on Ice Island ARLIS II, in *Arctic Drifting Stations*, AINA, Wash., D.C., pp. 439-458.
- Kutschale, H., 1968. Long-range sound propagation in the Arctic Ocean, in *Arctic Drifting Stations*, AINA, Wash., D.C., pp. 281-295.
- Kutschale, H. Surface waves from sources at depth in a multilayered liquid-solid half space with numerical computations for CW and pulse propagation in the Arctic SOFAR channel (in preparation).
- Kutschale, H. The phase integral method applied to long-range sound propagation in the Arctic Ocean (in preparation).
- Kutschale, H. Long-range sound propagation in the Arctic Ocean: A comparison of experiments with theory (in preparation).
- Prentiss, D.D., and J.I. Ewing, 1963. The seismic motion of the deep ocean floor. *Bull. Seism. Soc. Am.*, vol. 53(4), pp. 765-781.

- Shaver, R., and K. Hunkins, 1964. Arctic Ocean geophysical studies: Chukchi Cap and Chukchi Abyssal Plain. Deep-Sea Res., vol. 11, pp. 905-916.
- Ewing, M., K. Hunkins, and E. Thorndike, 1969. Some unusual photographs in the Arctic Ocean, Marine Tech. Soc. Journal.
- Thurber, D.L., G. Mathieu and K. Hunkins. Natural radiocarbon and fission products in Arctic Ocean water (in preparation).
- Van Donk, J. and G. Mathieu, 1969. Oxygen isotope compositions of foraminifera and water samples from the Arctic Ocean, J. Geophys. Res., vol. 74, pp. 3396-3407.

TECHNICAL REPORTS:

Issued under Contract Nonr 266(82)

Heirtzler, J.R., May 1963. Simultaneous geomagnetic measurements on an ice island surface and 1000 feet below. Tech. Rept. No. 2, CU-2-63-Nonr 266(82).

Prentiss, D., E. Davis and H. Kutschale, June 1965.

Natural and man-made ice vibrations in the central Arctic Ocean in the frequency range from 0.1 to 100 cps. Tech. Rept. No. 4, CU-4-65-Nonr 266(82).

Walker, J.C.G., March 1964. Geomagnetic observations in the Arctic Ocean: Drift Station ARLIS II, June 3 to August 21, 1962. Tech. Rept. No. 3, CU-3-64-Nonr 266(82).

Yearsley, J.R., Sept. 1966. Internal waves in the Arctic Ocean. Tech. Rept. No. 5, CU-5-66-Nonr 266(82).

ENCYCLOPEDIA ARTICLES AND OTHER

- Hunkins, K., 1966. Drifting Ice Stations in The Encyclopedia of Oceanography, ed. by R. Fairbridge, Reinhold, N.Y. pp. 232-3.
- Hunkins, K., and P.A. Kaplin, 1966. The Chukchi Sea in The Encyclopedia of Oceanography, ed. by R. Fairbridge, Reinhold, N.Y., pp. 191-196.
- Hunkins, K., and H. Kutschale, 1968. Seismic experiments on sea ice in International Dictionary of Geophysics ed. by S. Runcorn, Pergamon Press.

Security Classification

DOCUMENT CONTROL DATA - R & D

(Security classification of title, body of abstract and indexing annotation must be entered when the overall report is classified)

1. ORIGINATING ACTIVITY (Corporate author) Lamont-Doherty Geological Observatory of Columbia University		2a. REPORT SECURITY CLASSIFICATION Unclassified	
		2b. GROUP Arctic	
3. REPORT TITLE Studies in Marine Geophysics and Underwater Sound from Drifting Ice Stations			
4. DESCRIPTIVE NOTES (Type of report and inclusive dates) Final Report			
5. AUTHOR(S) (First name, middle initial, last name) Kenneth L. Hunkins, Henry W. Kutschale, John K. Hall			
6. REPORT DATE September 1969		7a. TOTAL NO. OF PAGES 102	7b. NO. OF REFS 49
8a. CONTRACT OR GRANT NO. NONR 266 (82)		9a. ORIGINATOR'S REPORT NUMBER(S)	
b. PROJECT NO. Code No. 8100		9b. OTHER REPORT NO(S) (Any other numbers that may be assigned this report)	
c.			
d.			
10. DISTRIBUTION STATEMENT Reproduction of this document in whole or in part is permitted for any purpose of the U. S. Government			
11. SUPPLEMENTARY NOTES		12. SPONSORING MILITARY ACTIVITY Office of Naval Research	
13. ABSTRACT The detailed drift of T-3 from May 1962 to June 1969 is plotted from over 9000 celestial and satellite fixes processed entirely by digital computer. Over 14,000 km of precision depth profiles show detailed topography of parts of the Northwind Ridge, Chuckchi Rise, Mendeleev Ridge, Alpha Cordillera, Wrangel Plain, Canada Plain, and Chuckchi Plain. Over 4,500 km of continuous seismic reflection profile show sediment thicknesses of about 1 km on the ridges to more than 3.5 km under Wrangel Plain. Over 49,000 magnetic and 10,000 gravity measurements have helped to delineate regional geologic structure and crustal movements. The sound scattering layer in the Arctic was discovered on precision depth recordings. Long-range sound propagation in the Arctic SOFAR channel is described by ray and normal mode theory. The normal mode treatment for the channel bounded above by a rough ice sheet is in remarkably good agreement with acoustic signatures from distant explosions. The Ekman current spiral was verified. This is the first quantitative verification of Ekman's theory in any deep ocean. The first observations of seismic noise on the Arctic Ocean floor were made aboard ice island ARLIS II. The continuous vertical oscillation of the ice was investigated. The Arctic wave spectrum contrasts with that of other oceans because the spectral peak due to sea and swell is absent. The			

DD FORM 1473 (PAGE 1)

S/N 0102-014-6600

Security Classification

